Journal of Hazardous Materials 476 (2024) 135188

Contents lists available at ScienceDirect

Journal of Hazardous Materials

journal homepage: www.elsevier.com/locate/jhazmat

Stress responses of the seagrass *Cymodocea nodosa* to environmentally relevant concentrations of pharmaceutical ibuprofen: Ecological implications

Virginia Menicagli [a,1], Monica Ruffini Castiglione [a,b,c,1], Emily Cioni [d,1], Carmelina Spanò [a,c,1], Elena Balestri [a,b,*], Marinella De Leo [b,d], Stefania Bottega [a], Carlo Sorce [a,c,1], Claudio Lardicci [b,c,e,1]

[a] Department of Biology, University of Pisa, via L. Ghini 13, 56126 Pisa, Italy
[b] Center for Instrument Sharing University of Pisa (CISUP), University of Pisa, Lungarno Pacinotti 43-44, 56126 Pisa, Italy
[c] Center for Climate Change Impact, University of Pisa, Via Del Borghetto 80, 56124 Pisa, Italy
[d] Department of Pharmacy, University of Pisa, Via Bonanno Pisano 33, 56126 Pisa, Italy
[e] Department of Earth Sciences, University of Pisa, via S. Maria 53, 56126 Pisa, Italy

HIGHLIGHTS

- Effects of seawater contamination by IBU on *Cymodocea nodosa* plants were assessed.
- IBU was detected in the seawater growth medium but not inside plant tissues.
- IBU altered specialized metabolite production and caused oxidative stress.
- IBU damaged photosynthetic machinery, especially PSII, at high concentration.
- Exposure to high IBU amounts may reduce seagrass resilience to other stressors.

GRAPHICAL ABSTRACT

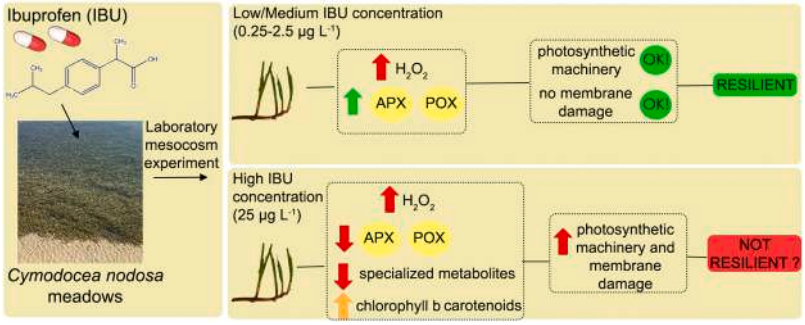

ARTICLE INFO

Keywords:
Ibuprofen
Oxidative stress
Photosynthetic efficiency
Resilience
Seagrass

ABSTRACT

Pharmaceuticals like ibuprofen (IBU) entering marine environments are of great concern due to their increasing consumption and impact on wildlife. No information on IBU toxicity to seagrasses is yet available. Seagrasses form key habitats and are threatened worldwide by multiple stressors. Here, the responses of the seagrass *Cymodocea nodosa* to a short-term exposure (12 days) to environmentally realistic IBU concentrations (0.25–2.5-25 μg L^{-1}), both at organism (plant growth) and sub-organism level (oxidative status, photosynthetic efficiency, and specialized metabolites production), were assessed in mesocosm. Chemical analyses to detect the presence of IBU and its metabolites in seawater and plants were also performed. IBU did not affect plant growth but caused physiological alterations which varied in severity depending on its concentration. Concentrations of 0.25 and 2.5 μg L^{-1} resulted in oxidative stress, but an increased antioxidant enzyme activity enabled plants to tolerate stress. A concentration of 25 μg L^{-1} caused greater oxidative stress, reduced antioxidant enzyme activity and specialized

* Correspondence to: University of Pisa, Department of Biology, Via Derna 1, 56126 Pisa, Italy.
E-mail address: elena.balestri@unipi.it (E. Balestri).
[1] These authors equally contributed.

https://doi.org/10.1016/j.jhazmat.2024.135188
Received 17 April 2024; Received in revised form 6 July 2024; Accepted 10 July 2024
Available online 15 July 2024

metabolites production, and impaired photosynthetic machinery functioning (particularly PSII). IBU was detected in seawater but not in plants suggesting no bioaccumulation. These findings indicate that *C. nodosa* could not withstand high IBU stress, and this could reduce its resilience to additional environmental stressors.

1. Introduction

The presence of active pharmaceutical ingredients as well as of their metabolites and degradation products in marine environments is an issue of increasing global concern due to their potential adverse effects, both in isolation and in combination with other stressors including climate changes (e.g., ocean acidification and warming and eutrophication), on organisms and ecosystems [1-9]. Seagrass meadows are considered one of the most valuable ecosystems in the world providing multiple services, such as nursery habitat and food source for many organisms, carbon sequestration, coastal protection, and improved water quality [10,11]. Seagrasses cover large coastal areas from sub-Artic to tropical regions also in proximity to urban and industrial effluents and are exposed to a wide range of contaminants including pharmaceuticals (Phs) [12-16]. These latter can continuously enter coastal environments through various point and nonpoint sources (e.g., urban and hospital wastewater treatment plant effluents, water bodies, animal husbandry and aquacultures; [3,9]). Due to their systemic use, continuous input, and lack of effective removal technologies, Phs are present in the marine environment in concentrations ranging from ng L^{-1}- μg L^{-1} [17,3,18]. Up to 600 Phs have been detected in seawater and marine sediments [3,19]. Some of them have been included in the European Water Framework Directive "Watch-list" as potentially harmful, but a strict and comprehensive regulation is still lacking [20]. The occurrence of Phs in marine animals, like mollusks, crustaceans, and fish, as well as in primary producers, like macroalgae and seagrasses, has been reported [21,22,15,23,24]. However, current information on their toxicity is mostly referred to few specific animal taxa and target species [25-32].

No studies have yet addressed the effects of Phs on seagrasses. This is a relevant knowledge gap since these habitat-forming species can cope with environmental changes, but multiple anthropogenic and climate change stressors, including pollutants, ocean acidification and heat waves, are likely to reduce their resilience [33-36,9]. Some seagrasses like *Zostera marina* L., *Posidonia oceanica* L. Delile and *Cymodocea nodosa* (Ucria) Ascherson are considered biological indicators of marine environmental quality due to their capacity to respond to a wide range of pollutants like herbicides, petrochemicals, and heavy metals present in sediments and in the water column [37,38,16]. For example, *C. nodosa,* which is one of the most widespread seagrasses in the Mediterranean, can bioaccumulate heavy metals and metal nanoparticles [39-41]. However, the exposure of this pioneer plant to silver and titanium dioxide nanoparticles as well as to micro- and nanoplastics can cause oxidative stress, leaf growth impairment, and changes in photosynthetic efficiency [42-46]. Similar alterations have been observed in *C. nodosa* plants exposed to environmentally occurring concentrations of an endocrine disrupting compound, bisphenol A, largely used in the chemical industry [47,48].

One of the most frequently detected Phs in coastal seawaters is the non-steroidal anti-inflammatory drug Ibuprofen (hereafter IBU). This contaminant has received an increasing attention in the recent years due to its extensive use during the COVID-19 pandemic [25,49,50]. Its estimated annual global consumption overcomes 10,000 metric tons, but a higher consumption and consequent release into coastal habitats is expected in the future [51,52]. IBU is considered a pseudo-persistent pollutant (i.e., a degradable compound that is constantly present in the environment because of its continuous introduction; [53]). It can enter wastewaters both in its original form (i.e., the parent compound 2-(4-Isobutylphenyl) propionic acid) and as its biotransformation products after consumption by humans or animals [54]. In wastewater effluents, IBU can reach concentrations up to 1673 μg L^{-1}, and lower levels (36.8 μg L^{-1}) have been observed in the receiving water bodies [55-59]. In freshwater, IBU can undergo degradation within a few days (half-life of 12 days) through several mechanisms like photolysis, reaction with •OH and with the triplet states of chromophoric dissolved organic matter [60-62]. Since IBU is a weak acid (pKa = 4.91) characterized by a relatively high solubility in water and an intermediate hydrophobicity, it can be potentially taken up by roots of vascular plants inhabiting riparian ecosystems [63,64]. Species like *Typha angustifolia* L., *Phragmites australis* (Cav.) Trin. ex Steud., and *Salix alba* L. can also metabolize and degrade this pollutant via detoxifying reactions involving specific enzymes (e.g., cytochrome P450 monooxygenase, glycosyltransferase, and glutathione-S transferase; [64-66]).

IBU concentrations in coastal surface seawaters range on average from 1.5 to 2.5 μg L^{-1}. Lower concentrations (up to 1 ng L^{-1}) are present in the open sea due to dilution effects and degradation (Table 1; [67-69, 18,30,70]). At seawater pH (pH 8.2) IBU can be transformed from the neutral to the anionic form [3], and its sorption on sediment is low resulting in concentrations in the range of ng L^{-1} in marine substrates [3, 71]. The few available information on the effects of IBU on marine photosynthetic organisms is based on studies performed using concentrations exceeding those commonly detected in marine environments, thus making it difficult to assess its actual environmental impact. Moreover, contrasting results emerged from these studies. For example, adverse effects, such as a decreased growth rate, oxidative stress, and changes of the photosynthetic pathway functioning, have been observed in the marine diatom *Pheodactylum tricornutum* Bohlin following exposure to IBU concentrations in the range of 100–300 μg L^{-1} [31]. Instead, no effects on the growth have been reported in the brown macroalga *Fucus vesiculosus* L. exposed to higher (up to 10,000 μg L^{-1}) IBU concentrations [72,73]. Such discrepancy in results may arise from differences at level of biological organization (unicellular *vs.* multicellular) and sensitivity between the investigated species, as well as among experimental conditions (e.g., exposure duration and temperature). Seagrasses largely differ from marine algae and other vascular plants inhabiting terrestrial environments or freshwaters showing peculiar physiological and morphological adaptations (e.g., regulation of osmotic pressure, presence of aerenchyma, and absence of stomata) to stressful marine conditions [74]. Given the global importance of seagrasses, understanding the effects of IBU on their development and resilience is crucial and may contribute to develop more effective management strategies.

The aim of this study was to evaluate the potential impact of IBU concentrations environmentally relevant for the Mediterranean on the performance of the seagrass *C. nodosa* by using mesocosms providing near-natural conditions. This species was selected because of its occurrence in shallow coastal areas including estuaries, its fast-growth rate, and its capacity to respond to environmental changes through morphological and physiological adaptations [94-99,44]. Specifically, the effects of a short-term exposure (12 days) of plants to different IBU concentrations using a multidisciplinary approach involving measurements both at organism level (morphological and growth traits) and sub-organism level (quali-quantitative specialized metabolites content, oxidative stress markers, antioxidant enzyme activity, and photosynthetic pigments and efficiency) were evaluated. Chemical analyses to detect the presence of IBU and its metabolites in plants and their growth medium were also performed.

Table 1
Summary of concentrations of Ibuprofen detected in coastal seawater, estuary seawater, and open seawater across the globe by previous studies.

Study site	Matrix	Concentration (ng L^{-1})	Reference
Indian Ocean, Singapore	coastal seawater	2.2 – 9.1	[75]
Indian Ocean, Singapore	coastal seawater	41 – 121	[76]
Indian Ocean, Kuwait	coastal seawater	22-4206	[77]
Indian Ocean, South Africa	coastal seawater	0 – 170	[78]
Indian Ocean, South Africa	coastal seawater	90	[79]
Pacific Ocean, Taiwan	coastal seawater	2.5 – 57.1	[80]
Pacific Ocean, Taiwan	coastal seawater	0 – 12.1	[81]
Pacific Ocean, California, USA	coastal seawater	12	[82]
Pacific Ocean, California, USA	coastal seawater	0 – 30	[83]
Red Sea, Saudi Arabian	coastal seawater	46.2-508.7	[84]
Atlantic Ocean, Brazil	coastal seawater	326 - 2094	[85]
Atlantic Ocean, Portugal	coastal seawater	0 – 222	[86]
Mediterranean, Greece and Turkey	coastal seawater	35	[82]
Mediterranean, Spain	coastal seawater	0 – 1219.7	[67]
Mediterranean Sea, Israel	coastal seawater	7.5	[82]
Mediterranean, North Adriatic Sea	coastal seawater	70	[82]
Mediterranean, Ionic Sea	coastal seawater	2.7-2550	[87]
Mediterranean, France	coastal seawater	1700	[70]
Mediterranean, Spain	coastal seawater	16	[88]
Sea of Marmara, Turkey	coastal seawater	15-2130	[89]
Baltic Sea, Germany	coastal seawater	109	[82]
Barents Sea, Norway	coastal seawater	0 – 0.7	[90]
North Sea, UK	estuary seawater	24.9-6297	[91]
North Sea, UK	estuary seawater	8-928	[92]
Atlantic Ocean, Portugal	estuary seawater	9-28	[93]
Atlantic Ocean, Spain	estuary seawater	0-1219.7	[67]
Atlantic Ocean, Spain	open seawater	0-32.3	[67]
Mediterranean, Italy	open seawater	0.049-1.14	[69]
Mediterranean, Italy	open seawater	0.063-1.08	[68]

2. Materials and methods

2.1. Chemicals

Standard IBU (CAS number 15687–27-1) was purchased from Sigma Aldrich, Germany (purity ≥ 98 %). The physico-chemical properties of IBU are reported in Table S1. A stock solution of IBU (10 mg L^{-1} in ethanol) was prepared just before the experiment began and stored temporarily (a few hours) in the laboratory at room temperature (18 °C) in darkness. Ultra High-Performance Liquid Chromatography (UHPLC) grade methanol, water, formic acid, and the standards rutin (≥ 98 % purity) and chicoric acid (≥ 95 % purity) were purchased from Merck KGaA (Darmstadt, Germany). Catechin standard was previously isolated and characterized by 1D- and 2D NMR, and HR-MS techniques in authors laboratory from other plant extracts. All the analytical grade solvents were acquired from VWR (Milano, Italy).

2.2. Plant material and experimental set-up

In May 2023, *C. nodosa* plagiotropic rhizome fragments were harvested in a shallow site (0.5 m) located in the Ligurian Sea (Italy, 43°22′55.66″N, 10°26′7.05″E). Fragments were transported to the laboratory and cut into experimental plant units (n = 60) of homogenous size (7.05 ± 0.08 cm, rhizome length; 4.18 ± 0.09 shoot number; 0.71 ± 0.43 root number; mean ± SE). Before the experiment, mesocosms (n = 60) consisting of glass culture vessels (0.5 L) containing natural seawater (NSW, pH = 8.13 ± 0.03, salinity = 38.03 ± 0.03 PSU) and a layer (3 cm) of washed and oven-sterilized sediment (silica sand, grain size 0.5–1 mm, density 1.6 g mL^{-1}, and less than 0.01 % of organic matter content) were set up. NSW was provided by INVE Aquaculture Research Center of Rosignano Solvay and filtered as described in Menicagli et al. [44]. A commercial NPK fertilizer (Cifo, 20–10-10 N-P-K, 0.44 g L^{-1}) was added in each mesocosm to sustain plant growth. A single plant unit was introduced in each mesocosm, and all mesocosms were kept in a culture chamber under controlled conditions in the range of those experienced by the species at the time of collection (temperature = 20 ± 1 °C, light intensity of 110–150 μmol m^{-2} s^{-1} photosynthetic photon flux density provided by LED lamps, and 12/12 h light/dark regime) for 7 days to allow each plant to acclimate.

After the plant acclimatization, the NSW in each mesocosm was entirely renewed, and the mesocosms were randomly assigned to one of the three nominal IBU concentrations (0.25 μg L^{-1} or Low, 2.5 μg L^{-1} or Medium, 25 μg L^{-1} or High) and control (0 μg L^{-1} or no IBU). These concentrations were within the range of those detected in European coastal waters [69,18,30,70]. They were achieved by dissolving appropriate aliquots of the IBU stock solution in the NSW added to each mesocosm. For each of the four treatments there were 15 mesocosms each containing one plant, thus in total there were 15 replicate plants per treatment. Ten out of these plants were left undisturbed and used at the end of the experiment for the analysis of the morphological and growth traits, the content of specialized plant metabolites and IBU (and its metabolites), and the evaluation of oxidative stress markers, antioxidant enzyme activity, and photosynthetic pigment production) as described in Fig. 1. The remaining five plants were monitored at different times (0, 1, 5 and 12 days after the exposure) for photosynthetic efficiency measurements (Fig. 1). Before assigning the plants to the IBU treatments, their morphological variables (number of shoots per plant, average number of leaves per shoot, length of the longest leaf on the apical shoot, and rhizome length) were recorded. Additional mesocosms (n = 12) were set up as described above, but no plant was introduced inside them. They were randomly attributed to each of the four IBU treatments (3 replicates per each treatment) and used as blanks. Thus, in total there were 72 mesocosms (Fig. 1). All the mesocosms were kept in the culture chamber under the same environmental conditions imposed during the acclimatization period. The NSW in each mesocosm was entirely renewed after 7 days, and aliquots of the IBU stock solution were added according to the nominal concentrations. The mesocosms were then kept in the growth chamber for 5 more days, thus the overall plant exposure to IBU lasted 12 days. This period was considered long enough to appreciate macroscopic plant growth changes. Indeed, *C. nodosa* produces 1–2 leaves per month and has a rhizome elongation rate up to 0.25 cm day^{-1} in the period May-June [96,100-102]. This period was also within the range of those used in previous studies assessing the effects of different contaminants on *C. nodosa* (8–12 days; [42-44,46]). During the experiment, the mesocosms were daily reallocated spatially in the growth chamber to avoid any possible position effects on plant growth. Physical/chemical variables (pH, conductivity, and the redox potential) of NSW were monitored every two days by using a multi-parameter meter (HI98194, Hanna Instruments). NSW loss due to evaporation was replaced by addition of MilliQ water. At the end

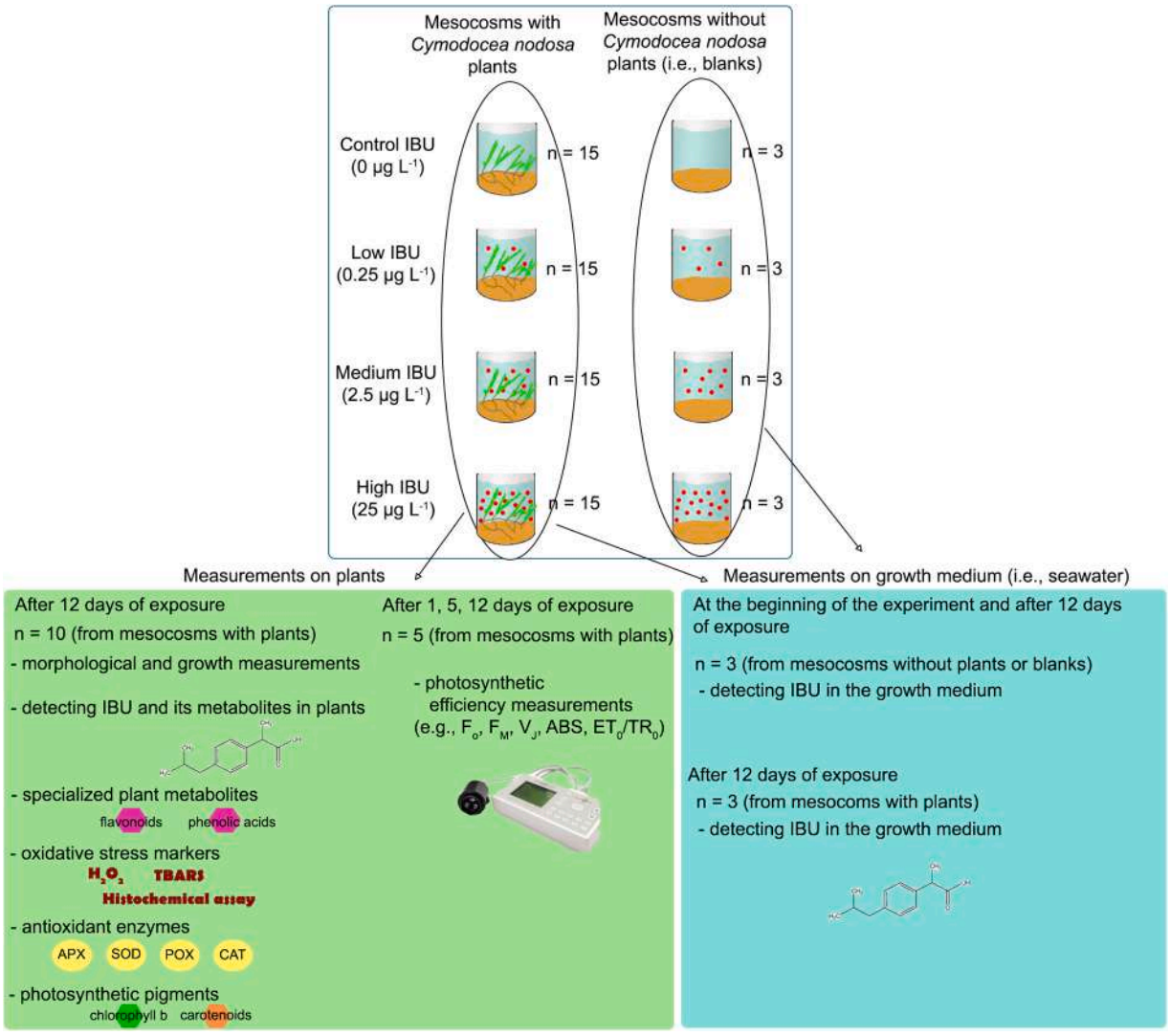

Fig. 1. Flow chart of the experiment.

of the experiment, all plants were removed and analyzed as described in Fig. 1. NSW samples (40 mL) were also collected from each mesocosm at the end of the experiment (Fig. 1). The same volume of NSW was also collected from blanks both at the beginning and at the end of the experiment. Collected NSW samples (3 replicates per treatment) were stored at 4 °C for subsequent analysis of the presence of IBU (Fig. 1).

2.3. Plant morphological and growth traits

At the end of the experiment, the number of plants survived after each treatment was determined and their morphological variables were measured. The net change in shoot number for each plant was calculated as the difference between the number of newly produced shoots and that of dead shoots within the experimental exposure period. The net change in leaf number was calculated as the difference between the number of newly produced leaves and the number of detached leaves averaged across all the standing shoots present on each plant within the experimental exposure period. Leaf (or rhizome) elongation was calculated as the difference between the final length and the initial length of the longest leaf on the apical shoot (or the rhizome) over the initial length and expressed as a percentage.

2.4. Preparation of NSW and plant extract samples for chemical analyses

To determine the amount of IBU present in NSW, the collected samples were evaporated under vacuum (Buchi Rotavapor®, Milano, Italy) and the residues were partitioned with *n*-BuOH/H_2O (1:2 v/v) to remove salts and centrifuged for 5 min at 2710 × g. The *n*-butanol fractions were subjected to vacuum drying and finally dissolved in 100 µL of methanol for liquid chromatography (LC) coupled to mass spectrometry (MS) analyses. To determine the amount of IBU, and its main metabolites (hydroxyibuprofen, dihydroxyibuprofen, ibuprofen glucoside, and carboxyibuprofen) possibly produced by phase I and II metabolism of plants [64], a sample of biomass (1 g) from plants not exposed (control) or exposed to different IBU concentrations was used. The amount of specialized metabolites produced by the plants was also determined. The small plant size prevented us from assessing the distribution of IBU (and its metabolites) in the different organs (leaves, rhizomes and roots). Each plant sample was subjected to extraction with 5 mL of methanol for 15 min by ultrasonic bath LBS2 (Falc Instruments s.r.l., Treviglio, Italy) and finally centrifuged for 5 min at 2710 × g. The supernatants were transferred into vials to be injected into the LC-MS system.

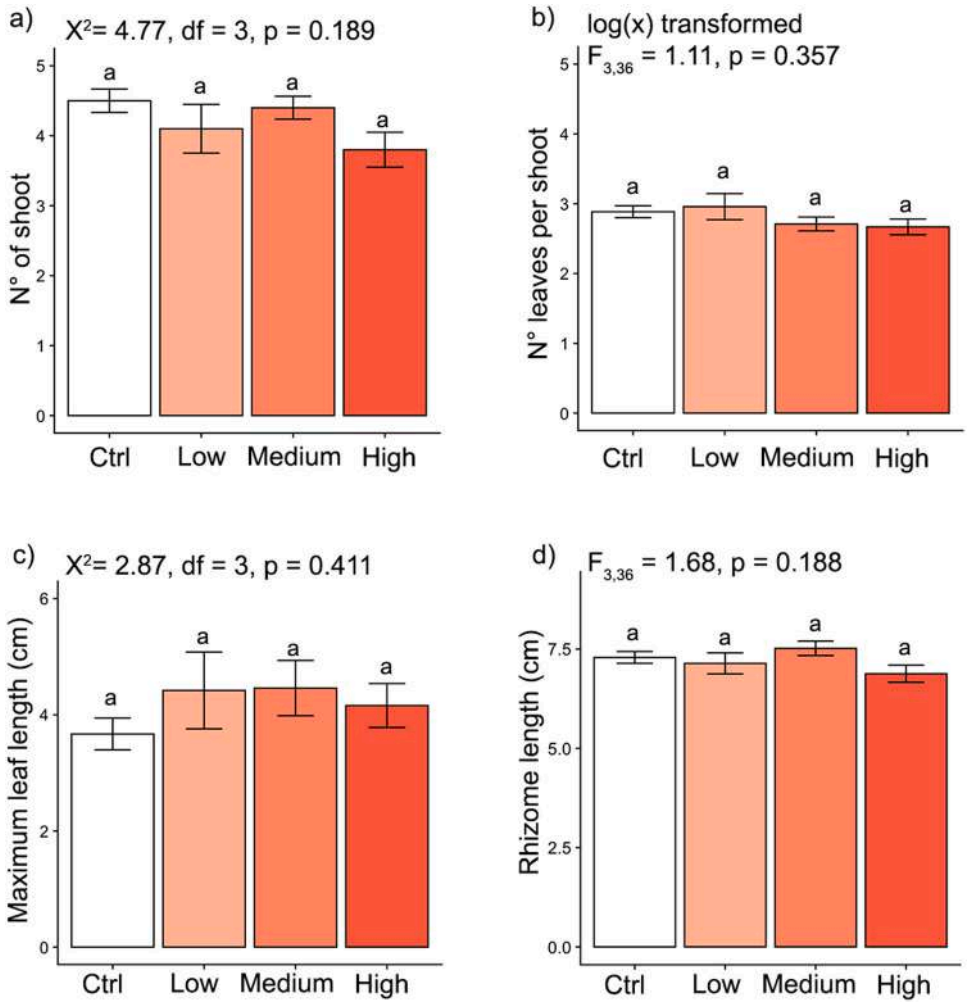

Fig. 2. (a) Initial number of shoots per plant, (b) average number of leaves per shoot, (c) maximum leaf length, and (d) rhizome length of *Cymodocea nodosa* plants assigned to different IBU concentrations (0 μg L^{-1} or control-Ctrl, 0.25 μg L^{-1} or Low, 2.5 μg L^{-1} or Medium, 25 μg L^{-1} or High) at the beginning of the experiment (i.e., before plant exposure to IBU). The results of statistical analyses are reported, and different letters denote significant differences ($p < 0.05$) among treatments. Mean ± SE.

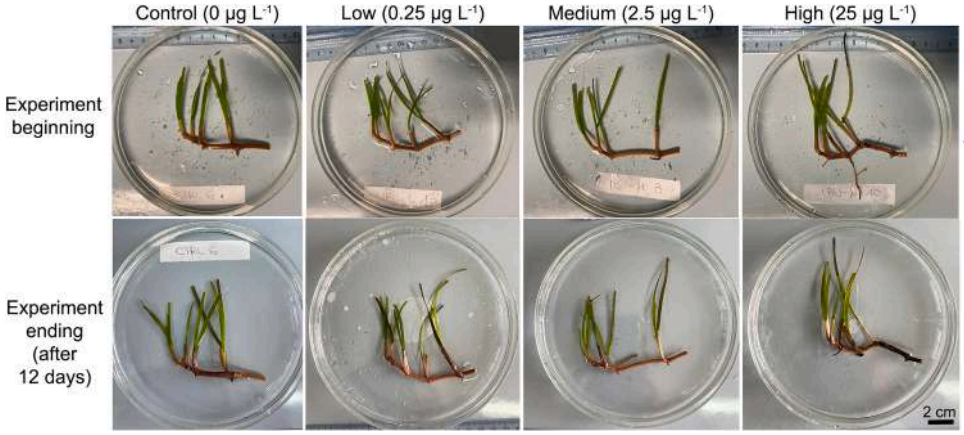

Fig. 3. *Cymodocea nodosa* plants exposed to different IBU concentrations (0 μg L^{-1} or control-Ctrl, 0.25 μg L^{-1} or Low, 2.5 μg L^{-1} or Medium, 25 μg L^{-1} or High) at the beginning and at the end of the experiment.

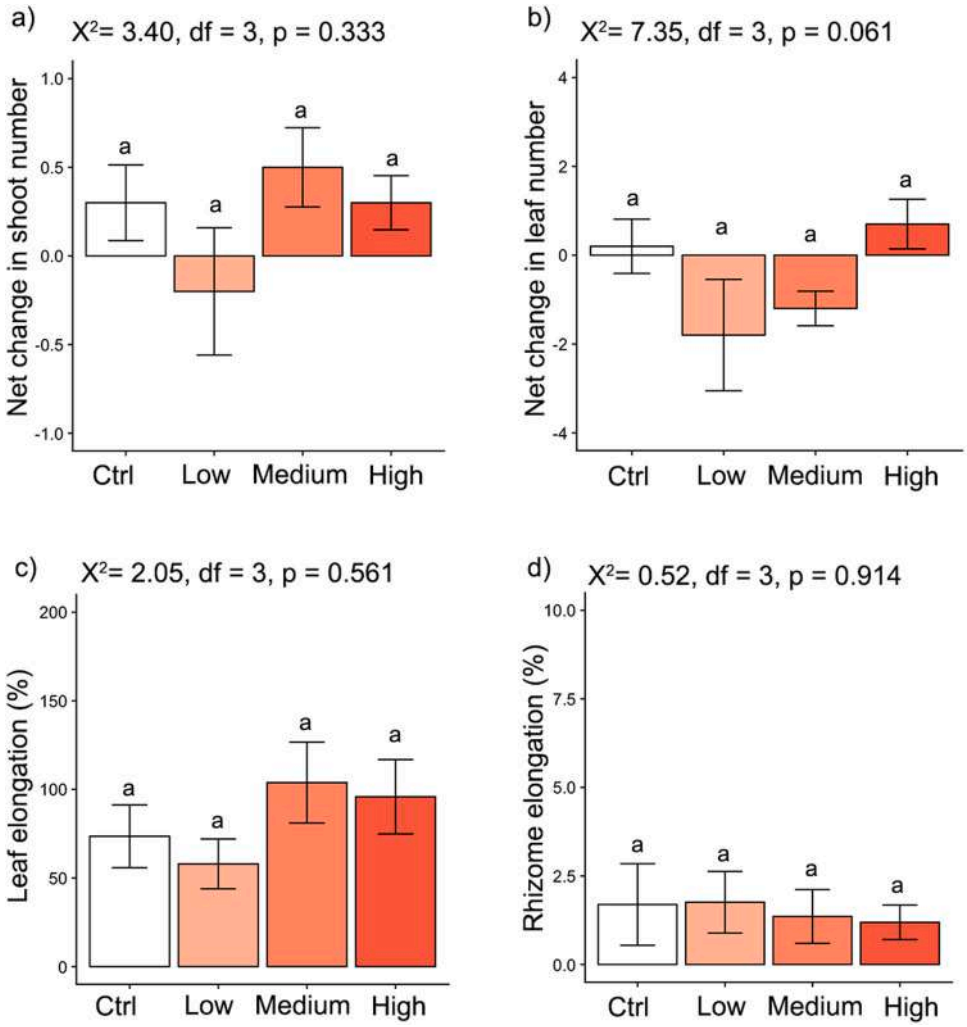

Fig. 4. (a) Net change in shoot number, (b) net change in leaf number, (c) leaf elongation, and (d) rhizome elongation of *Cymodocea nodosa* plants exposed to different IBU concentrations (0 μg L^{-1} or control-Ctrl, 0.25 μg L^{-1} or Low, 2.5 μg L^{-1} or Medium, 25 μg L^{-1} or High). The results of statistical analyses are reported, and different letters denote significant differences ($p < 0.05$) among treatments. Mean ± SE.

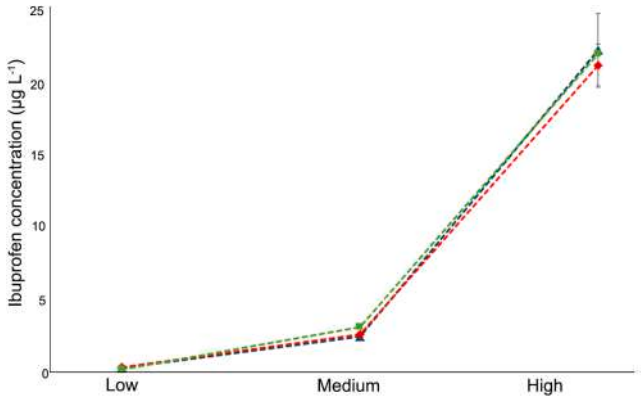

Fig. 5. Concentrations of IBU in NSW from mesocosms without *Cymodocea nodosa* plants (i.e., blanks) assigned to different IBU treatments (0.25 μg L^{-1} or Low, 2.5 μg L^{-1} or Medium, 25 μg L^{-1} or High) at the beginning (black dashed line) and at the end (green dashed line) of the experiment. Concentrations of IBU in NSW from mesocosms containing *C. nodosa* plants exposed to the three IBU treatments (red dashed line) at the end of the experiment are also reported. Mean ± SE.

2.5. Quali-quantitative liquid chromatography-high-resolution mass spectrometry (LC-HR-MS) analyses to detect IBU in NSW and plant samples, and evaluate plant specialized metabolite production

The solutions (5 μL) obtained from NSW and plant samples were individually injected into an UHPLC coupled with a diode array detector (DAD) and a high resolution (HR) Q Exactive Plus Orbitrap MS, equipped with an electrospray ionization (ESI) source and a hybrid quadrupole analyzer (Thermo Fischer Scientific Inc., Bremem, Germany). The chromatographic runs were performed by using a Kinetex® Biphenyl C-18 column (2.1 ×100 mm, 2.6 μm) equipped with a Security Guard™ Ultra Cartridge (Phenomenex, Bologna, Italy) at a flow rate of 0.5 mL min^{-1}. The autosampler and the column oven were maintained at a temperature of 4 °C and 35 °C, respectively. As a mobile phase, a mixture of HCOOH/H_2O 0.1 % v/v (solvent A) and HCOOH/MeOH 0.1 % v/v (solvent B) was chosen and a linear gradient was used, increasing from 5 to 80 % B in 20 min. The ESI-HR mass spectra were recorded in negative and positive ionization modes, operating in Parallel Reaction Monitoring (PRM) for IBU detection. Standard solutions of IBU were used as reference standards, with IBU detected both in negative and positive modes ($[M-H]^-$ at *m/z* 205.1228; $[M+H]^+$ at *m/z* 207.1376, Fig. S1). UV data were recorded in a range of 200–600 nm, using 254, 280 and 325 nm as preferential channels. Nebulization voltage of 3500 V, capillary temperature of 300 °C, sheath gas (N_2) 20 arbitrary

Table 2
Concentration of phenols (i.e., phenolic acids and flavonoids) found in the extracts of *Cymodocea nodosa* plants exposed to different IBU concentrations (0 μg L^{-1} or control-Ctrl, 2.5 μg L^{-1} or Medium, 25 μg L^{-1} or High). Different uppercase letters indicate statistical differences among treatments. FW = fresh weight; SD = standard deviation.

Peak	Compound	Concentration (μg g^{-1} FW ± SD) Ctrl	Medium	High
	Phenolic acids and derivatives			
2	Gallic acid	0.515 ± 0.1^{B}	0.25 ± 0.02^{B}	1.04 ± 0.02 ^{A}
3	Hydroxybenzoic acid	2.00 ± 0.2 ^{A}	2.67 ± 0.1 ^{A}	2.39 ± 0.8 ^{A}
4	Hydroxybenzoic acid derivative	52.7 ± 5 ^{A}	37.2 ± 4 ^{A}	7.16 ± 0.4^{B}
5	Dihydroxybenzoic acid hexoside	1.35 ± 0.1 ^{A}	1.24 ± 0.1 ^{A}	0.69 ± 0.05^{B}
6	Hydroxymethylbenzoic acid derivative	149 ± 10 ^{A}	91.7 ± 8^{B}	68.4 ± 7^{B}
7	Caftaric acid I	2.02 ± 0.03 ^{A}	2.03 ± 0.6 ^{A}	1.92 ± 0.4 ^{A}
10	Coutaric acid	2.37 ± 0.3 ^{A}	2.38 ± 0.3 ^{A}	1.61 ± 0.2 ^{A}
11	*p*-Dihydrocoumaric acid derivative	8.20 ± 0.7^{B}	14.3 ± 3 ^{AB}	23.1 ± 3^{A}
12	*p*-Coumaroyl hexoside I	2.77 ± 0.1 ^{A}	2.58 ± 0.1 ^{A}	0.75 ± 0.2^{B}
13	*p*-Coumaroyl hexoside II	5.76 ± 0.7 ^{A}	3.24 ± 0.1^{B}	0.70 ± 0.3 ^{C}
14	Feruloyltartaric acid	1.62 ± 0.2^{AB}	1.96 ± 0.1 ^{A}	1.05 ± 0.1^{B}
16	Feruloylhexoside	14.8 ± 0.3 ^{A}	12.8 ± 0.4^{B}	2.26 ± 0.6 ^{C}
17	*p*-Coumaric acid	1.43 ± 0.01^{B}	1.30 ± 0.1^{B}	3.85 ± 0.1 ^{A}
18	*p*-Dihydrocoumaric acid	13.3 ± 2 ^{A}	1.50 ± 0.7 ^{A}	19.0 ± 7 ^{A}
19	*p*-Coumaroylmalic acid	3.21 ± 0.2 ^{A}	1.74 ± 0.8 ^{AB}	0.66 ± 0.1^{B}
20	Chicoric acid	53.2 ± 3^{AB}	65.7 ± 8^{A}	38.6 ± 2^{B}
21	Caftaric acid II	2.20 ± 0.1^{AB}	3.32 ± 0.4 ^{A}	1.64 ± 0.1^{B}
23	Ferulic acid	3.32 ± 0.2 ^{A}	4.30 ± 0.7 ^{A}	2.60 ± 0.1 ^{A}
24	Feruloylmalic acid	3.45 ± 0.2 ^{A}	2.14 ± 0.4^{B}	2.23 ± 0.1^{B}
26	*p*-Coumaroylcaffeoyltartaric acid	15.9 ± 4 ^{A}	16.3 ± 3 ^{A}	6.01 ± 0.7 ^{A}
31	Caffeoylferuloyltartaric acid	10.9 ± 2 ^{A}	10.6 ± 2 ^{A}	8.15 ± 2 ^{A}
32	*p*-Dicoumaroyltartaric acid	5.36 ± 0.8^{AB}	6.13 ± 0.4 ^{A}	3.42 ± 0.4^{B}
38	Diferuloyltartaric acid	1.25 ± 0.1 ^{A}	1.16 ± 0.1 ^{A}	1.12 ± 0.02 ^{A}
	Flavonoids			
8	Catechin	46.0 ± 4 ^{A}	40.5 ± 3 ^{A}	38.2 ± 3 ^{A}
9	Procyanidin B-type dimer	28.8 ± 1 ^{A}	24.9 ± 6 ^{A}	11.4 ± 2 ^{A}
15	Epicatechin	1.89 ± 0.2 ^{A}	1.85 ± 0.4 ^{A}	1.13 ± 0.5 ^{A}
22	Rutin	5.84 ± 0.6^{B}	6.06 ± 0.5^{B}	9.44 ± 0.2 ^{A}
25	Quercetin hexoside	15.0 ± 0.9 ^{A}	14.4 ± 1 ^{A}	19.1 ± 2 ^{A}
27	Quercetin malonylhexoside	3.24 ± 0.3 ^{A}	3.30 ± 0.2 ^{A}	3.60 ± 0.1 ^{A}
28	Kaempferol hexoside	1.91 ± 0.3 ^{A}	1.62 ± 0.2 ^{A}	0.43 ± 0.1^{B}
29	Isorhamnetin rutinoside	55.6 ± 4 ^{A}	51.9 ± 7 ^{A}	32.0 ± 0.3 ^{A}
30	Isorhamnetin hexoside	226 ± 5 ^{A}	220 ± 16 ^{A}	144 ± 25 ^{A}
33	Naringenin hexoside	1.70 ± 0.2 ^{A}	1.33 ± 0.2 ^{A}	0.79 ± 0.04 ^{A}
35	Isorhamnetin acetylhexoside	30.4 ± 2 ^{A}	30.0 ± 4 ^{A}	9.14 ± 0.7^{B}
36	Isorhamnetin malonylhexoside	35.4 ± 2 ^{A}	34.9 ± 5 ^{A}	10.0 ± 0.9^{B}
39	Isorhamnetin	12.3 ± 1 ^{A}	9.65 ± 3 ^{A}	2.62 ± 0.3 ^{A}
	Total phenolic acids	357 ± 30	287 ± 33	198 ± 26
	Total flavonoids	464 ± 22	441 ± 47	282 ± 35
	Total phenols	821 ± 52	728 ± 80	480 ± 61

units, auxiliary gas (N_2) 3 arbitrary units, HCD (Higher-energy C-trap dissociation) of 18 eV were applied as ionization settings [103]. The limit of detection (LOD) and the limit of quantification (LOQ) for IBU were calculated basing on chromatograms obtained by triplicate injections of IBU methanol solutions at decreasing concentrations, performing serial dilutions from a 1 mg mL^{-1} mother stock solution. A calibration curve was constructed for quantitation using six different concentrations in a range 2.5 ng - 1 μg mL^{-1}, showing good linearity and correlation coefficient (R^2 = 0.9981). Differences in the concentration of IBU and its main metabolites among treatments were assessed by comparing the areas of the extracted ion peaks from the chromatograms obtained by LC-MS analyses.

For the analysis of specialized metabolites in plant extracts, a scan range of *m/z* 135–2000 was applied, recording MS both in full (70000 resolution, 220 ms maximum injection time) and data dependent-MS/MS scan (17500 resolution, 60 ms maximum injection time). Detected compounds were tentatively identified by comparing their chromatographic (retention times, t_R) and MS data (HR full and fragmentation mass spectra) with data reported in the literature, considering an accepted mass error < 5 ppm on the experimental molecular formula. The level of confidence for compound identification corresponds to level 3 of the system described by Schymanski et al. [104]. The specialized metabolites were also quantified by constructing calibration curves using reference standard for each class of compounds. Specifically, three pure external standards such as chicoric acid for phenolic acids, rutin for flavonoid glycosides, and catechin for (epi)catechin and their derivatives were used. Triplicate solutions of chicoric acid and rutin were prepared in a concentration range of 1.95–62.5 μg mL^{-1}, obtaining calibration curves with a good linearity over the entire range and R^2 equal to 0.999 and 0.998, respectively. Catechin calibration curve was prepared in a concentration range of 12.5–100 μg mL^{-1}, showing R^2 = 0.992. Xcalibur 4.1 software (Thermo Fisher Scientific Inc., Bremen, Germany) was used to process the acquired chromatographic profiles and MS^n (n = 1, 2 levels) spectra. Results were expressed as mean (μg g^{-1} of FW) ± standard deviation (SD).

2.6. Oxidative stress markers: hydrogen peroxide, thiobarbituric acid reactive substances and histochemical assay

In order to measure hydrogen peroxide (H_2O_2) concentrations in plants, leaves and rhizomes were homogenized in 50 mM phosphate buffer (pH 6.5), centrifuged, and the supernatant was mixed with 0.1 % titanium chloride in 20 % (v/v) H_2SO_4. The absorbance was read at 410 nm [105]. The concentration of H_2O_2 was determined using a standard curve and then expressed as micromoles per gram of fresh weight (μmol g^{-1} FW). The concentrations of thiobarbituric acid reactive substances (TBARS) were determined by measuring the absorbance at 532 nm after subtracting non-specific absorbance at 600 nm, and quantified as nmol g^{-1} FW, following homogenization and extraction of plant material [106].

For the histochemical assay, leaves of similar size and length were isolated and divided into tip and mid-leaf segments.H_2O_2 was detected histochemically by dipping leaf portions in a staining solution

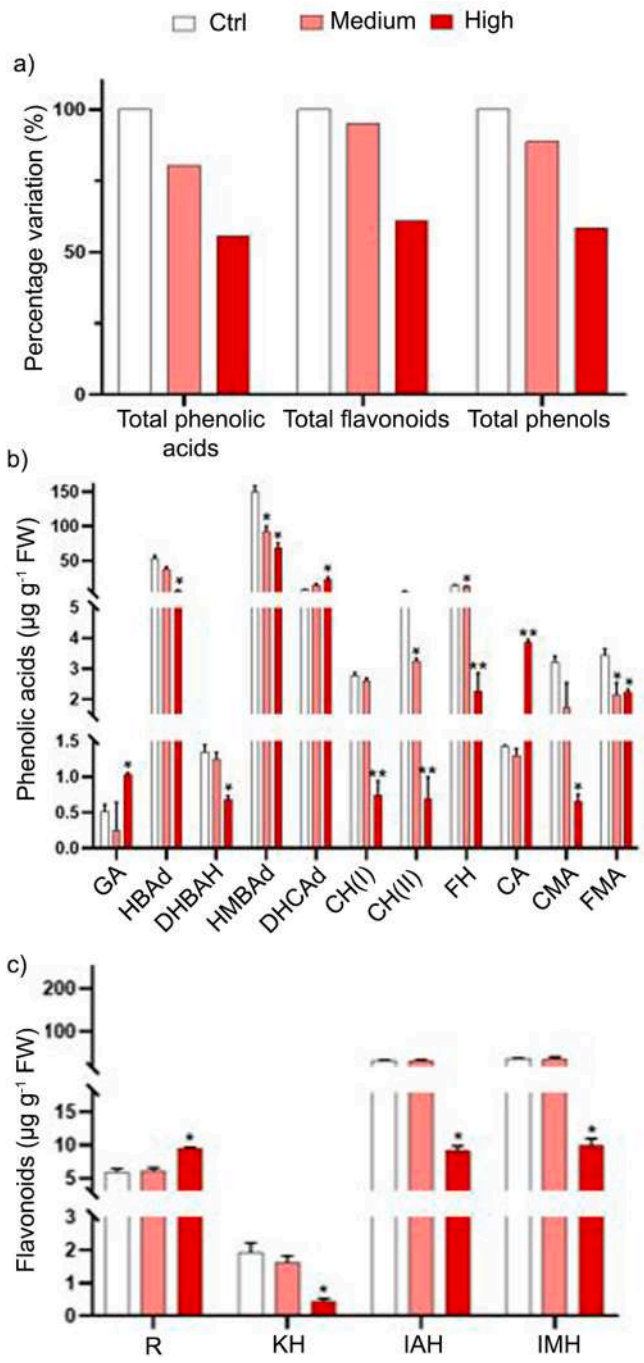

Fig. 6. Phenols identified in extracts of *Cymodocea nodosa* plants exposed to different IBU concentrations (0 µg L^{-1} or control-Ctrl, 2.5 µg L^{-1} or Medium, 25 µg L^{-1} or High): (a) percentage variation; (b) phenolic acids and (c) flavonoids differing significantly in amount from the control. GA = gallic acid; HBAd = hydroxybenzoic acid derivative; DHBAH = dihydroxybenzoic acid hexoside; HMBAd = hydroxymethylbenzoic acid derivative; DHCAd = *p*-dihydrocoumaric acid derivative; CH(I) and CH(II) = *p*-coumaroyl hexoside isomers; FH = feruloylhexoside; CA = *p*-coumaric acid; CMA= *p*-coumaroylmalic acid; FMA = feruloylmalic acid; R = rutin; KH = kaempferol hexoside; IAH = isorhamnetin acetylhexoside; IMH = isorhamnetin malonylhexoside. * = $p < 0.05$; * * = $p < 0.005$. Mean ± SD.

containing 1 mg mL^{-1} of 3,3′-diaminobenzidine (DAB) at pH 3.8, followed by vacuum infiltration for 20 min [107]. The samples were left overnight in the same solution, treated with 96 % ethanol for 60 min at 65 °C, and examined under a light microscope to assess the presence of brown precipitates. In situ determination of lipid peroxidation was conducted using Schiff's reagent (VWR Chemicals BDH) [44,108], which binds to free aldehyde groups, serving as a qualitative indicator of lipid peroxidation. Leaf segments were incubated with the dye for 60 min at room temperature, followed by bleaching in 96 % ethanol for 60 min at 65 °C and then examined under a light microscope to evaluate the development of a purple coloration. Histochemical analyses were performed using a Leitz Diaplan microscope, with images captured using a Leica DFC 420 camera. The probes used for the analyses were selected for their detectability with an optical microscope thus avoiding issues related to the red autofluorescence of chlorophyll.

Cross rhizome sections were prepared using a hand microtome. The detection of H_2O_2 within the rhizome slices was conducted according to Giorgetti et al. [109], utilizing Amplex UltraRed Reagent (Life Technologies, USA). Following staining, the slices were mounted in glycerol and examined using a fluorescence microscope with excitation/emission wavelengths of 568ex/681em nm. Lipid peroxidation levels were assessed using a fluorescence microscope by observing the change in fluorescence emission peak from red to green after staining with the BODIPY 581/591 C11 probe (Life Technologies, USA), as described by Spanò et al. [110]. Microscope evaluation involved acquiring both green (485ex/510em nm) and red fluorescence (581ex/591em nm) signals simultaneously and merging the two images. Fluorescence microscope analysis was carried out using a Leica DMLB microscope equipped with the appropriate excitation/emission filters, along with a Leica DFC7000 T camera.

2.7. Extraction of antioxidant enzymes from plants and determination of their activity

Antioxidant enzymes were extracted from plant samples in 100 mM potassium phosphate buffer (pH 7.5) as described in Spanò et al. [111]. The activity of ascorbate peroxidase (APX, EC 1.11.1.11) was measured by monitoring the decrease in absorbance at 290 nm (extinction coefficient of 2.8 mM^{-1} cm^{-1}) due to ascorbate oxidation [112]. A correction for the non-enzymatic oxidation of ascorbate by hydrogen peroxide (blank) was applied. Catalase (CAT, EC 1.11.1.6) activity was determined [113] and calculated using the extinction coefficient of 39.4 mM^{-1} cm^{-1}. A blank containing only the enzymatic solution was prepared. The guaiacol peroxidase (POX, EC 1.11.1.7) activity was determined by using 1 % guaiacol as substrate and measuring guaiacol oxidation by H_2O_2 at 470 nm (extinction coefficient of 26.6 mM^{-1} cm^{-1}), with one unit oxidizing 1.0 µmol guaiacol per minute [114]. The superoxide dismutase (SOD, EC 1.15.1.1) activity was determined as described in Spanò and Bottega [115]. One SOD unit was defined as the amount required to inhibit by 50 % the photoreduction of nitroblue tetrazolium, measured spectrophotometrically at 550 nm. All enzymatic activities were assessed at 25 °C and expressed as units per milligram of protein (U mg^{-1} protein). The protein quantification was conducted utilizing bovine serum albumin (BSA) as a standard [116].

2.8. Extraction and determination of plant photosynthetic pigments

Leaf chlorophylls (a, b, and total) and carotenoids were extracted and determined according to Spanò and Bottega [115]. Briefly, the leaves were homogenized in 80 % acetone, and the extracts were then centrifuged for 10 min at 6000 g at 4 °C. After collecting the supernatants, the pellets were resuspended and re-extracted with 80 % acetone until they became colorless. The combined supernatants were analyzed using a spectrophotometer at wavelengths of 645 nm, 663 nm, and 470 nm. Pigment contents were expressed as milligrams per gram of fresh weight (mg g^{-1} FW).

2.9. Chlorophyll a fluorescence transient kinetics

The analysis of the fast fluorescence kinetics was carried out four times: before IBU treatment (T0), and after one (T1), five (T5), and 12

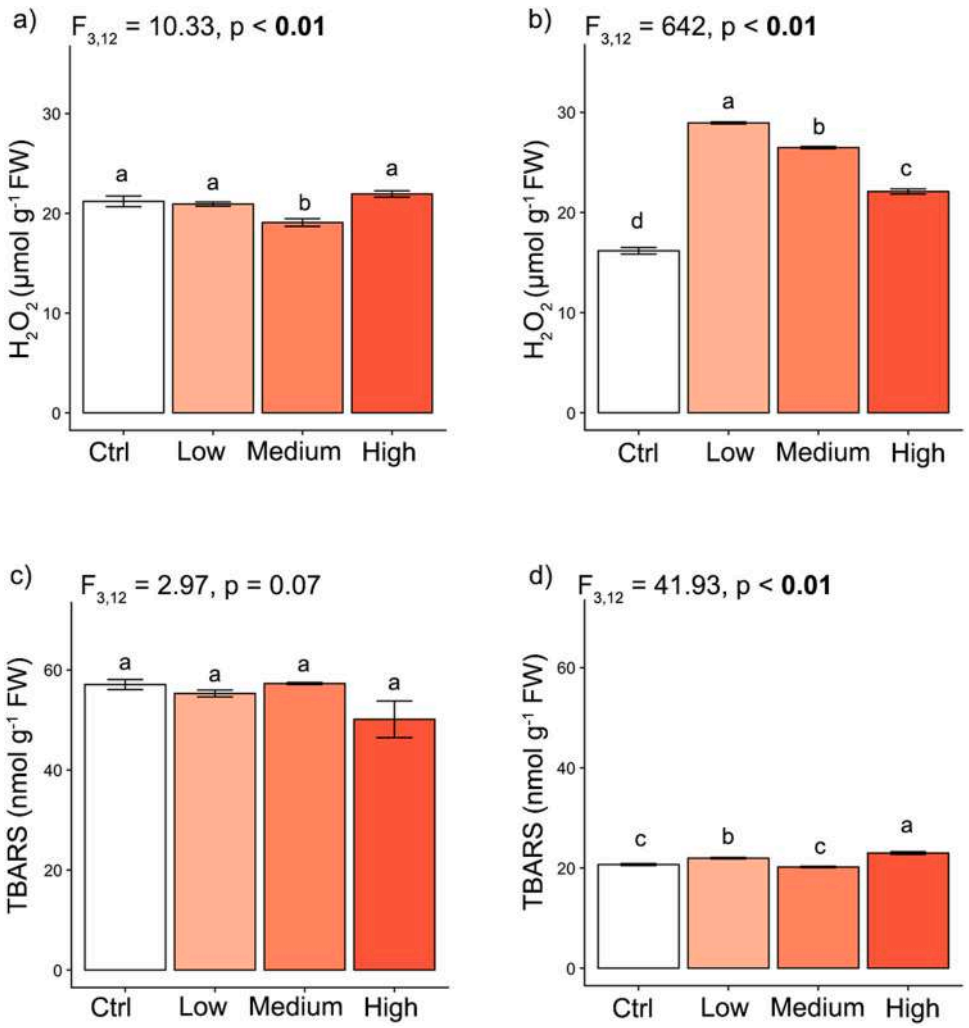

Fig. 7. Concentration of (a,b) hydrogen peroxide (H_2O_2) and (c,d) thiobarbituric acid reactive substances (TBARS) in rhizome (left column) and leaves (right column) of *Cymodocea nodosa* plants exposed to different IBU concentrations (0 µg L^{-1} or control-Ctrl, 0.25 µg L^{-1} or Low, 2.5 µg L^{-1} or Medium, 25 µg L^{-1} or High). The results of statistical analyses are reported, and different letters denote significant differences ($p < 0.05$) among treatments. Mean ± SE.

(T12) days of treatment. A Handy PEA fluorometer (Hansatech Instruments Ltd., Pentney, King's Lynn, UK) was used to record fluorescence. Before each measurement, the plants were acclimated to darkness for 30 min, then withdrawn from water and quickly blotted with paper to eliminate excess water. All operations were carried out in darkness with the aid of a dim diffuse light. Two leaf clips were applied to each plant (one clip for each shoot) and kept for 4 min to avoid interferences on fluorescence kinetic data resulting from exposure to such light source. Based on preliminary tests this time lapse had proven to be sufficient for the purpose. The values recorded from the two clips applied on each plant were averaged to yield a single replicate. Thus, five replicates were available for each treatment. After measurements, the plants were put back in the water. Chlorophyll a fluorescence (ChlF) was measured while the previously darkened clipped areas were exposed for 1 s to 3500 µmol photons m^{-2} s^{-1} (peak wavelength of 650 nm). Data were processed by PEA Plus software (Hansatech Instruments Ltd.), which carried out the analysis of the fast fluorescence kinetics or JIP test [117]. The JIP test parameters were computed using F_O, F_J, F_I, and F_M in addition to the ChlF values that were obtained at 50 µs, 100 µs, and 300 µs [118]. Table S2 contains a list of the parameters. To facilitate comparisons, JIP test parameters were reported as xControl values, that was, as ratios between treatment and control data, clustered according to their magnitudes. Only those parameters which significantly differed from controls were graphically shown.

2.10. Statistical analyses

The effects of the exposure of *C. nodosa* plants to IBU on morphological and growth traits, specialized metabolites, oxidative stress markers, antioxidant enzyme activity, photosynthetic pigments, and photosynthetic efficiency were assessed through a one-way analysis of variance (ANOVA, "GAD" package, [119]). Before performing ANOVAs, the normality and homoscedasticity of data were assessed by Shapiro–Wilk test and Cochran C test, respectively. Since some data did not meet ANOVA assumptions, they were analyzed by a Kruskal-Wallis test, the nonparametric analog to the one-way ANOVA. In case of a significant effect, a Tukey HSD post-hoc test was carried out following ANOVA to discriminate differences among tested IBU concentrations. For APX activity in leaves, a post hoc Dunn test was applied as it is the appropriate procedure following a Kruskal–Wallis test [120]. The statistical analyses were performed in R environment (version 3.5.2; R [121]) and by JMP® Pro 16.0.0 (SAS Institute Inc., Cary, NC, USA) software.

3. Results and discussion

3.1. Plant morphological and growth traits

Assessing survival and growth changes in seagrasses in response to abiotic stressors and pollutants is considered the most ecologically

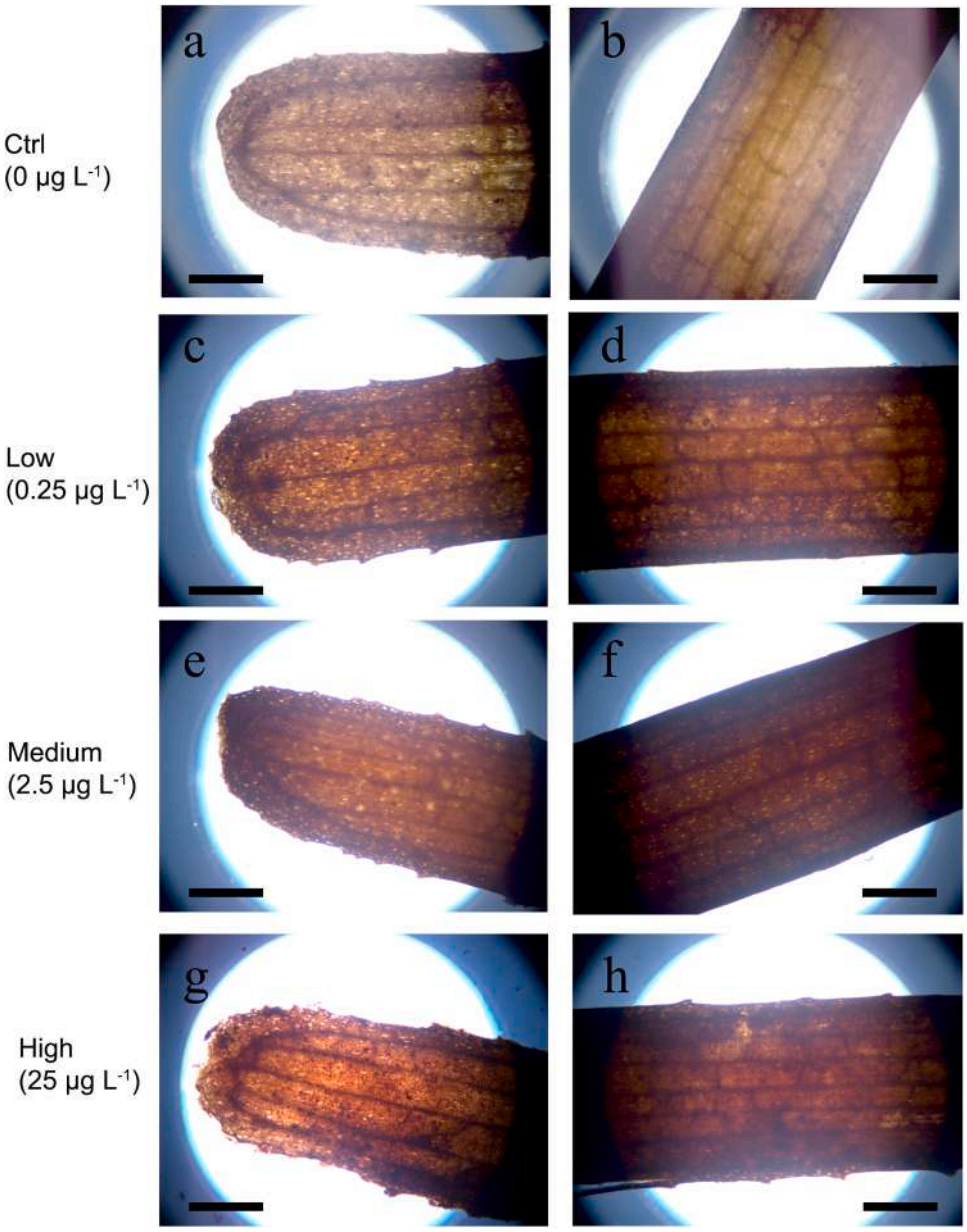

Fig. 8. Representative images of leaf portions of *Cymodocea nodosa* plants processed to histochemical detection of H_2O_2 by DAB staining following their exposure to different IBU concentrations (0 µg L^{-1} or control-Ctrl, a-b; 0.25 µg L^{-1} or Low, c-d; 2.5 µg L^{-1} or Medium, e-f; 25 µg L^{-1} or High, g-h). Tip-leaf segments (left column) and mid-leaf segments (right column). Scale bar = 1 mm. The dark brown colour indicates the presence of hydrogen peroxide.

relevant endpoint. But early warning symptoms of stress, like physiological and biochemical changes, can anticipate macroscopic changes associated to permanent plant damage. In our study, no difference in shoot number, average number of leaves per shoot, length of the longest leaf, and rhizome length of plants attributed to different IBU concentrations was detected before their exposure to IBU (Fig. 2). All plants survived until the end of the experiment, and no macroscopic changes in plant morphological and growth traits associated to plant damage were observed (Figs. 3, 4). Previous studies assessing the effects of the exposure of the marine macroalga *F. vesiculosus* and the diatom *P. tricornutum,* as well as of vascular plants like *Lemna minor* L. and *S. alba*, to IBU concentrations within the range of those applied in our study have reported no growth inhibition effects [122,65,72,123,31, 73]. Our results also agree with those of a previous study in which the exposure of *C. nodosa* to silver nanoparticles did not affect leaf and rhizome elongation although it induced oxidative stress [46]. However, the occurrence of adverse effects of IBU on *C. nodosa* growth on a longer term might be not excluded based on the physiological alterations described in the below sections.

3.2. *Quali-quantitative liquid chromatography-high-resolution mass spectrometry (LC-HR-MS) analyses to detect IBU in NSW and plant samples, and evaluate plant specialized metabolite production*

3.2.1. *Detection of IBU in NSW and plant samples*

The LC-MS analysis revealed the presence of linearly decreasing concentrations of IBU in NSW samples from blanks (i.e., mesocosms without plants) supplemented with high, medium, and low concentrations, and no IBU in NSW blank samples with no added IBU both at the beginning and at the end of the experiment. The IBU amounts measured in IBU-supplemented NSW samples from mesocosms containing *C. nodosa* plants at the end of the experiment were consistent with those found in blanks for all tested concentrations (Fig. 5). Instead, the presence of IBU or its metabolites was not detected in *C. nodosa* extracts.

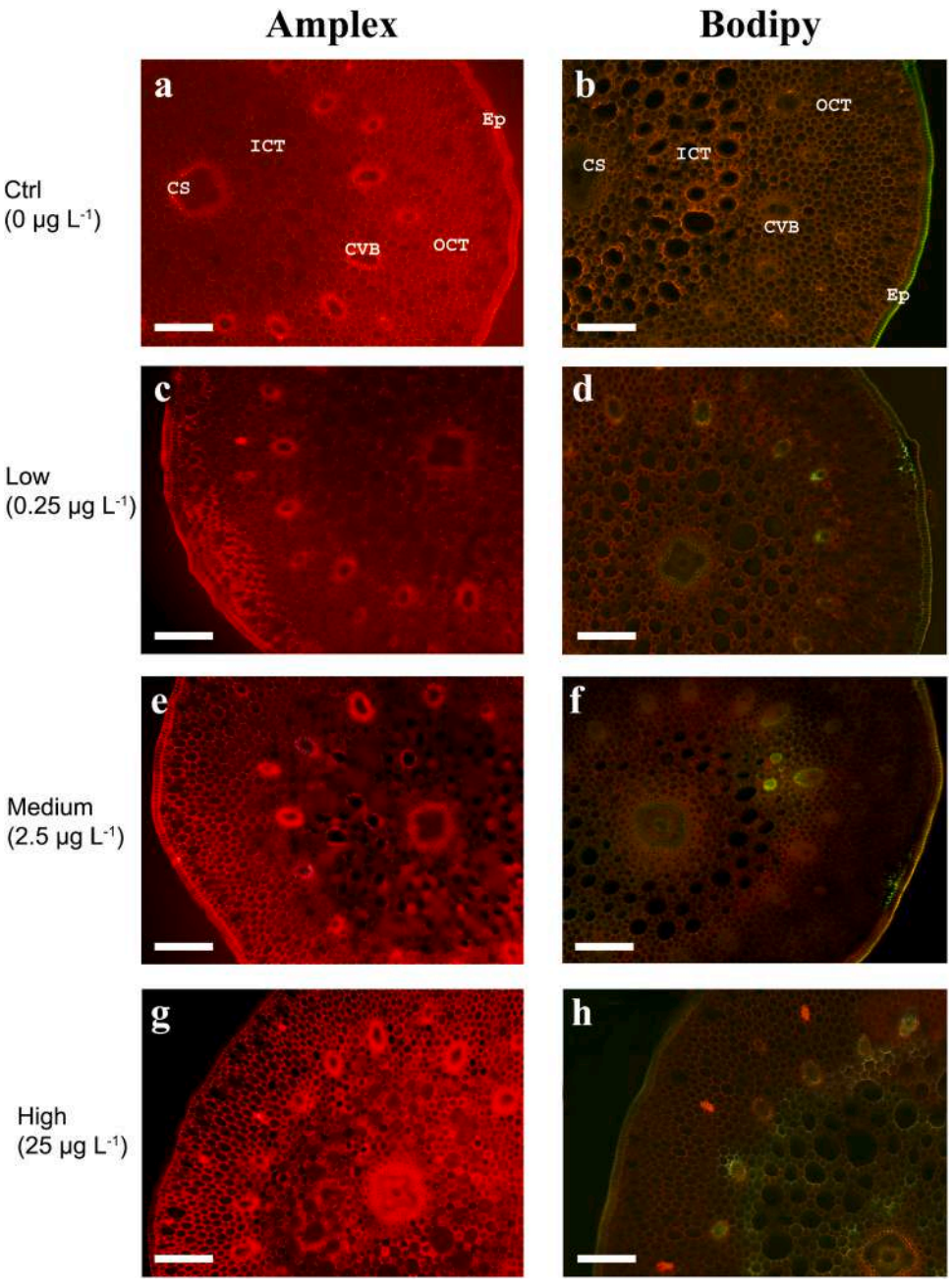

Fig. 9. Representative images of rhizome cross sections of *Cymodocea nodosa* plants processed to histochemical detection of oxidative stress markers following their exposure to different IBU concentrations (0 µg L^{-1} or control-Ctrl, a-b; 0.25 µg L^{-1} or Low, c-d; 2.5 µg L^{-1} or Medium, e-f; 25 µg L^{-1} or High,g-h). Amplex probe (H_2O_2 indicator, images left) and Bodipy probe (lipid peroxidation indicator, images right). Ep= Epidermis; OCT= Outer Cortical Tissues; CVB= Cortical Vascular Boundles; ICT= Inner Cortical Tissues; CV= Central stele. Scale bar = 100 µm.

These findings suggest no relevant IBU uptake by plants. However, an IBU uptake below the level of the instrumental LOD (>1 µg L^{-1}) and LOQ (>2.5 µg L^{-1}) cannot be excluded.

3.2.2. *Quali-quantitative analyses of plant specialized metabolites*

The chemical fingerprints of control and IBU treated plants were superimposable (Fig. S2), suggesting that the metabolite production was not qualitatively influenced by IBU. A total of 39 compounds were tentatively identified (Table S3): one tricarboxylic acid, 23 phenolic acids and derivatives, 13 flavonoids, and two dihydrochalcones. This finding provides novel valuable information about the chemical compounds produced by *C. nodosa*, since only few phenols have been identified so far in this species [124-126]. Apart from citric acid (**1**), all these compounds belong to the large class of phenols, the most represented specialized metabolites in plants involved in many physiological activities [127]. Phenolic acids were represented by gallic acid (**2**), hydroxybenzoic acid (**3**) with their derivatives (**4**-**6**), and several hydroxycinnamic acids such as *p*-coumaric (**17**) and ferulic (**23**) acids, together with their derivatives resulting from ester bond with malic or tartaric units and glycosidic linkage with monosaccharides. Caffeic acid derivatives, such as caftaric (**7**) and chicoric (**20**) acids were also identified. The identification of these molecules by MS data was based on the presence in the fragmentation mass spectra of diagnostic product ions generated by the loss of a CO_2 molecule (−44 u) [128], a tartaroyl (−149 u) or a maloyl residue (−132 u) due to the cleavage of acyl moiety, and a hexose unit (−162 u) due to the cleavage of glycosidic

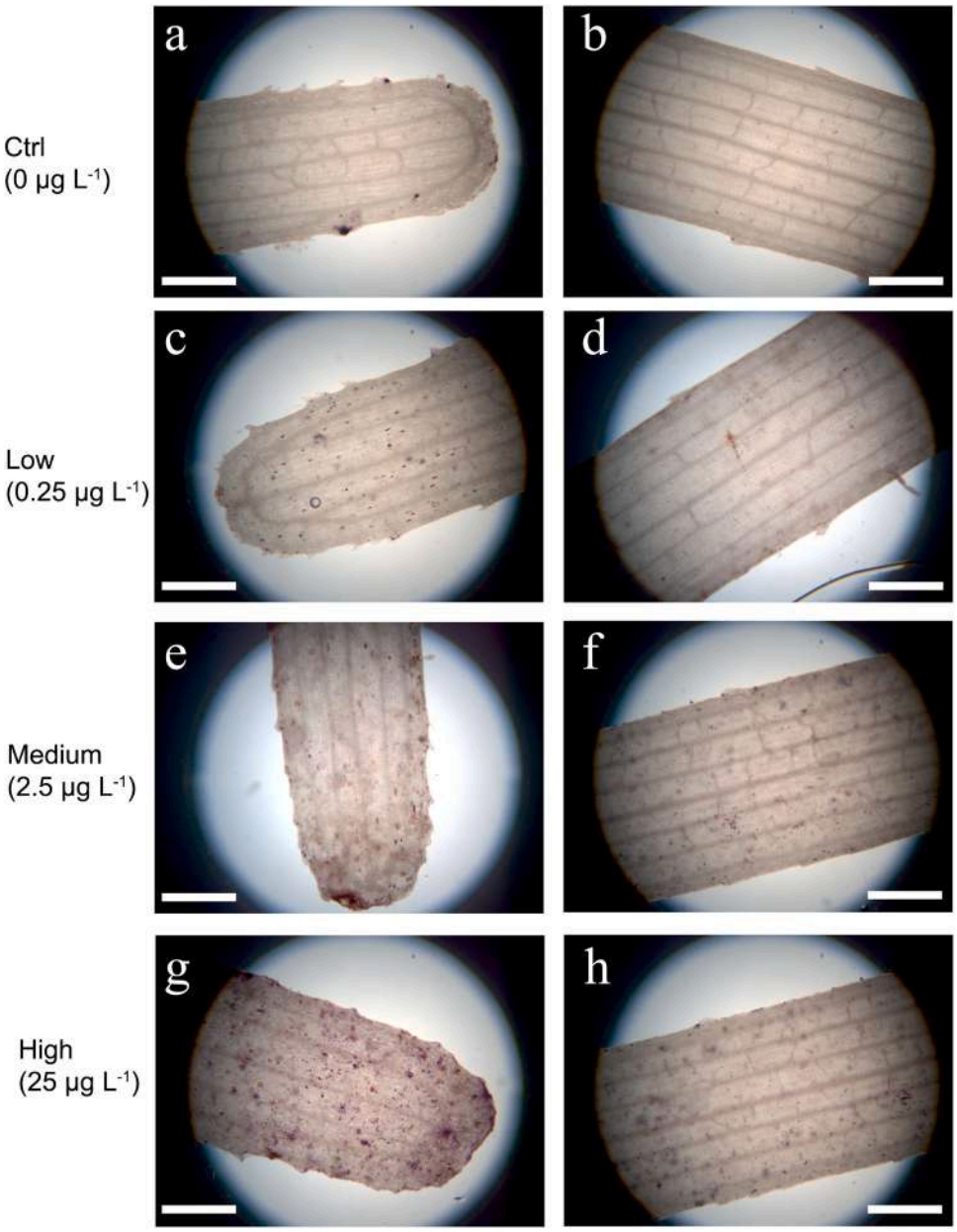

Fig. 10. Representative images of leaf portions of *Cymodocea nodosa* plants processed to histochemical detection of lipid peroxidation by Schiff's reagent staining following their exposure to different IBU concentrations (0 µg L^{-1} or control-Ctrl, a-b; 0.25 µg L^{-1} or Low, c-d; 2.5 µg L^{-1} or Medium, e-f; 25 µg L^{-1} or High, g-h). Tip-leaf segments (left column) and mid-leaf segments (right column). Scale bar = 1 mm. The development of purple coloration indicates oxidative membrane damage.

linkage [125,129]. Compounds **4**, **6** and **11** were not completely annotated, but the presence of base ion peaks at *m/z* 137.02, 151.04, 165.06, respectively, suggested that these molecules are hydroxybenzoic, hydroxymethylbenzoic, *p*-dihydrocoumaric acid derivatives [130]. Interestingly, other hydroxycinnamic acids than chicoric acid (**20**) and caftaric acid (**7**) previously isolated in *C. nodosa* [124] were here found in great structural diversity, free or as conjugates. As an example, compounds **26** and **31** differed from caftaric acid for the presence of an additional *p*-coumaroyl and feruloyl moieties, respectively. Our LC-MS analysis also identified a higher number of flavonoids compared to that reported in the available literature [124,125]. Flavonoids appeared for the most part in form of mono- or disaccharides of quercetin, kaempferol, naringenin, and isorhamnetin, as deduced by the detection in the MS/MS experiments of the aglycon portion at *m/z* 300.03, 285.04, 271.06, and 315.04, respectively [131-133]. Catechin (**8**), epicatechin (**15**), and a procyanidin B-type dimer (**9**), typically found in barks of terrestrial plants [103,134] were also detected. Finally, the analysis revealed the presence of two dihydrochalcones, phloretin (**37**) and its glucoside form phlorizin (**34**), exhibiting ESI-MS^2 peaks in agreement with data reported in the literature [135].

The quantitative analysis revealed a significant difference in the content of some specialized metabolites among plants exposed to high IBU concentration and controls (Table 2). In general, total phenolic acids and flavonoids were almost halved in the plants exposed to IBU (480 ± 61 µg g^{-1} FW ± SD) compared to controls (821 ± 52 µg g^{-1} FW ± SD) (Fig. 6a). The decrease in the concentration of total phenolic compounds is consistent with results of previous studies showing a lower production in *C. nodosa* plants in response to salinity stress and bisphenol A [48, 136]. In our study the content of the phenolic acids, *p*-coumaroylmalic acid (**19**), *p*-coumaroyl hexoside I (**12**) and II (**13**) significantly decreased in plants exposed to medium or high IBU concentrations compared to control (Fig. 6b,c). Instead, gallic acid (**2**), *p*-coumaric acid

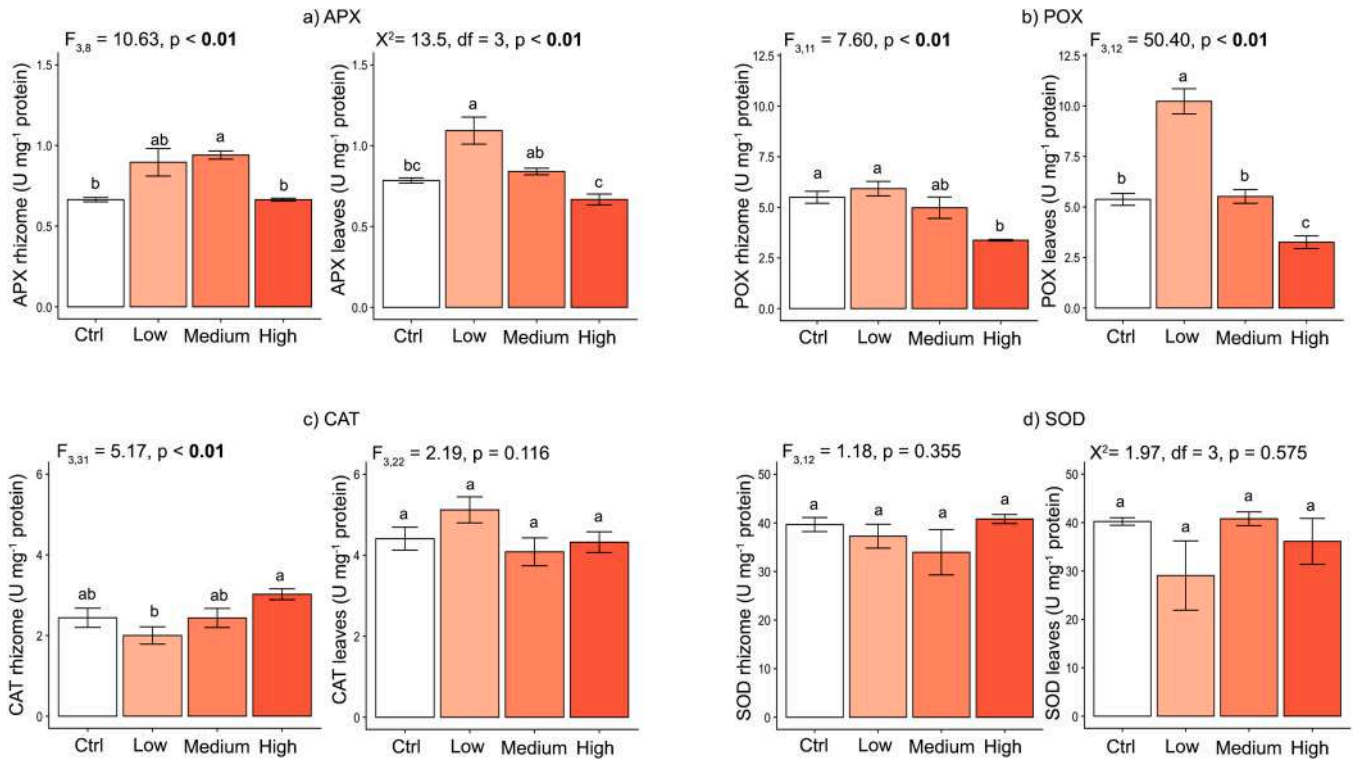

Fig. 11. Activity of the antioxidant enzyme (a) APX, (b) POX, (c) CAT, and (d) SOD detected in rhizomes and leaves of *Cymodocea nodosa* plants exposed to different IBU concentrations (0 μg L^{-1} or control-Ctrl, 0.25 μg L^{-1} or Low, 2.5 μg L^{-1} or Medium, 25 μg L^{-1} or High). The results of statistical analyses are reported, and different letters denote significant differences ($p < 0.05$) among treatments. Mean ± SE.

(**17**) and *p*-dihydrocoumaric acid derivative (**11**) showed a significant increase in plants treated with high IBU concentration. Among flavonoids, only rutin (**22**) increased in plants treated with high IBU concentration. Previous studies demonstrated that in plants the expression of genes involved in the biosynthetic pathways of some specialized metabolites can be modulated, either upregulated or downregulated, by abiotic stresses. This can often lead to an overproduction of antioxidant compounds, such as rutin, gallic acid and *p*-coumaric acid, that increase stress tolerance [137-139]. However, evidence also shows that the concentration of some specialized metabolites can decrease following the exposure of plants to abiotic stresses [140] . Thus, the significant changes in the production of these specialized metabolites observed in our study could be considered as a response of *C. nodosa* to the stressful conditions induced by IBU. Overall, our findings agree with the results of a previous study on other seagrass species reporting the presence of a wide range of simple phenols and flavonoids, key compounds involved in plant defense and response to biotic/abiotic stress [141].

3.3. *Oxidative stress markers, antioxidant enzyme activity and photosynthetic pigments*

Previous studies have shown that IBU, like other Phs, can induce an oxidative burst in the terrestrial plants by increasing ROS production [142]. An overproduction of ROS can cause damage to cell structure and macromolecules and trigger the activation of the antioxidant machinery [143,144]. In our study, among ROS, H_2O_2 was selected because it plays a key role in plant responses to oxidative stress , and its monitoring is considered as a reliable indicator of the severity of environmental stress [143]. The leaves of plants exposed to IBU had significantly higher levels of H_2O_2 than those of controls, and the H_2O_2 amount increased with the decreasing of IBU concentration (Fig. 7). This trend is not unusual, and a non-typical dose-effect relationship for oxidative stress markers has also been observed in plant responses to other contaminants [109]. It can partly be explained by the dual role of hydrogen peroxide: it acts both as a signal molecule for oxidative stress and as a participant in various physiological processes [145]. An overproduction of H_2O_2 was also found previously in *C. nodosa* leaves following the exposure to ecologically relevant concentrations of bisphenol A, silver nanoparticles, and nanoplastics [48,44,46] indicating that different environmental contaminants can induce oxidative stress also in this seagrass. Biochemical results are consistent with histochemical ones, showing an intense H_2O_2-dependent colorimetric response in leaves (Fig. 8). The leaves of plants exposed to IBU were more intensely dark-brown stained compared to controls, both in the tips and in the mid-leaf segments, with no specific staining pattern, demonstrating a general disturbance. A slightly more prominent disturbance in the middle portion of the leaf was observed in plants exposed to the medium and high IBU concentration (Fig. 8f,h).

In our study, the concentration of H_2O_2 in the rhizome of plants exposed to the low and high IBU treatment did not differ significantly from that of controls, and in plants exposed to the medium IBU concentration it was significantly lower (Fig. 7). These findings align with the results of a study on the terrestrial plant *Vigna unguiculata* L., showing no significant increase in the concentration of this ROS in plants exposed to the lowest IBU concentration used (400 ppm, [142]).

Applying the histochemical approach, which allows direct visualization of H_2O_2 in the rhizome, the staining linked to the red fluorescent probe used (Amplex Ultrared) showed specific localization patterns within the organ tissues (Fig. 9). In control plants, the red signal of the fluorescent probe was uniformly distributed, and the epidermis and cortical vascular bundles were slightly more intensely colored (Fig. 9a). In plants exposed to low IBU concentration, the signal extended to part of the outer cortical tissue (Fig. 9c), and in plants exposed to the medium and high concentration this tissue became overall intensely positive to the probe (Fig. 9e,g). Furthermore, in plants exposed to medium IBU concentration and especially in those at the highest one, even the inner cortical tissue with large air spaces and the central stele was positive for the dye (Fig. 9e,g). These results indicate that IBU can influence tissue-

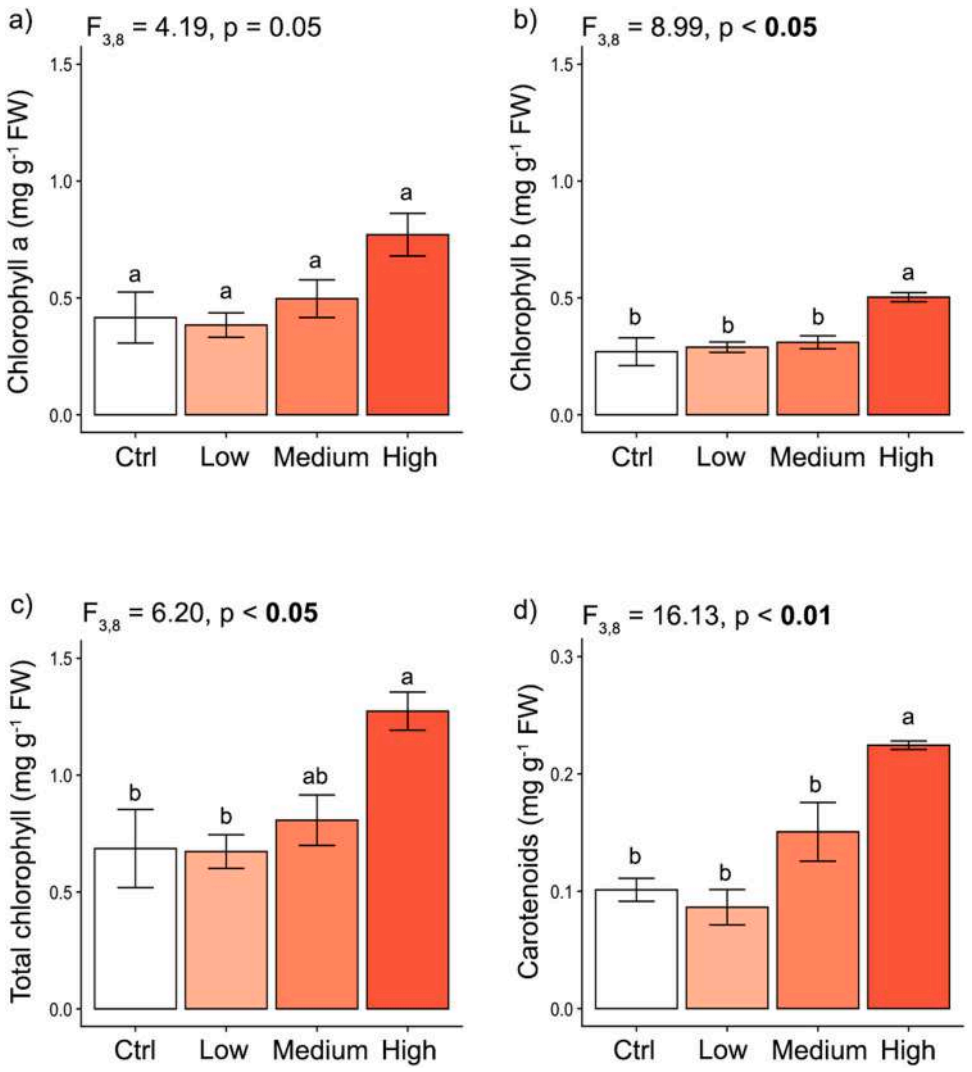

Fig. 12. Concentration of (a) chlorophyll a, (b) chlorophyll b, (c) total chlorophyll, and (d) carotenoids measured in *Cymodocea nodosa* plants exposed to different IBU concentration (0 μg L^{-1} or control-Ctrl, 0.25 μg L^{-1} or Low, 2.5 μg L^{-1} or Medium, 25 μg L^{-1} or High). The results of statistical analyses are reported, and different letters denote significant differences ($p < 0.05$) among treatments. Mean ± SE.

specific reactions depending on the concentration despite not changing the overall H_2O_2 levels in the rhizome. Overall, these findings suggest that the response of *C. nodosa* to environmental stress can vary according to the organ, and that the leaves were more sensitive than the rhizome to IBU. This greater effect may be related to the direct contact of leaves with the IBU in seawater.

Excess of ROS can often result in oxidative damage, and TBARS can be used as an indirect measurement of membrane oxidative damage. Here, a greater oxidative damage was detected in *C. nodosa* leaves at the high IBU concentration than in controls (Fig. 7) in accordance with results obtained histochemically with the Schiff's reagent (Fig. 10). An increase in oxidative damage was also reported in previous studies examining the response of *C. nodosa* to bisphenol A [48]. As observed for H_2O_2, IBU did not affect TBARS concentration in the rhizome (Fig. 7), but the histochemical determination revealed different patterns according to IBU concentration (Fig. 9). In control plants, only the epidermis was positive for Bodipy staining, while in plants exposed to low and medium IBU concentration the staining was also present in the vascular cortical bundles (Fig. 9d, f) and extended to the internal cortical tissues in those at the high concentration (Fig. 9h). Both biochemical and histochemical data indicate that IBU can induce oxidative damage even when administered at environmentally relevant concentrations. These results are consistent with a previous study on the diatom *P. tricornutum* exposed to IBU in which an overall increment in lipid peroxidation estimated as TBARS was recorded [31].

To counteract oxidative injury plants have evolved a complex antioxidant machinery, including enzymes such as POX, CAT, APX and SOD, which are directly involved in ROS detoxification [146]. In our experiment, differences in the activity of antioxidant enzymes, except that for SOD, were recorded in rhizome and leaves (Fig. 11). This is in contrast with the results of a previous study in which significant differences for SOD activity and not for APX and CAT activities, were detected in *P. tricornutum* after the exposure to IBU concentrations comparable to those tested here [31]. Such discrepancy could be related to the different duration of the experiment (96 h *vs.* 12 days), to the timing of activation of the antioxidant enzymes, and, most notably, to the different photoautotrophic organisms used. In our study, the APX and POX activities measured in leaves progressively decreased from the low to the high IBU concentration (Fig. 11). The reduced activity of antioxidant enzymes at the high concentration of different stressors is not unusual in *C. nodosa*, as reported for SOD following the exposure to the highest tested concentration of bisphenol A [48]. The reduced activity of APX and POX could be due to the inability of plants to activate antioxidant defense mechanisms efficiently and cope with ROS when exposed to such a high IBU concentration, in accordance with the highest oxidative damage, in terms of TBARS, detected in this condition. In contrast, CAT activity did

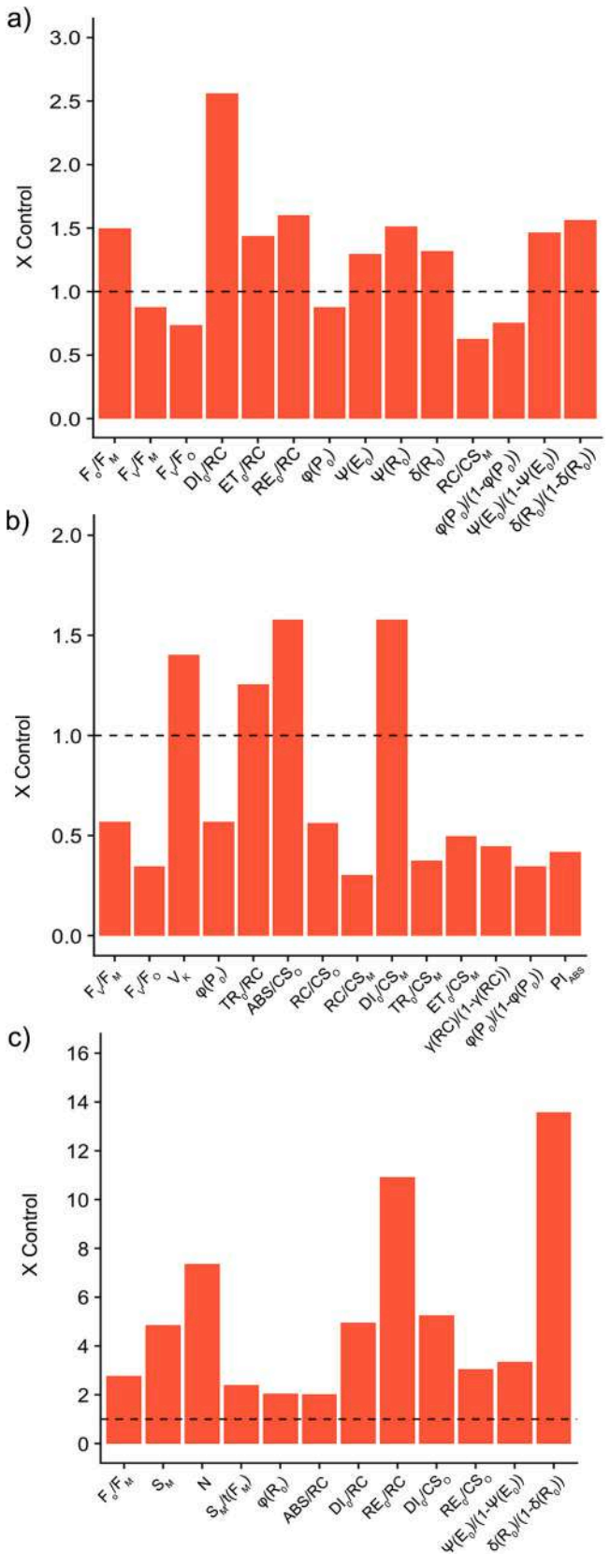

Fig. 13. Effects of the exposure to 25 μg L^{-1} IBU for (a) 5 days and (b, c) 12 days in dark-adapted *Cymodocea nodosa* leaves. The bar plots report the parameters of JIP test (described in Table S2), normalized to the values of the control, which were set as one. Dashed lines = control (value = 1).

not differ among treatments (Fig. 11). The different pattern of CAT and APX activity is often noted in the literature and could be due to their different affinity for the substrate (i.e., H_2O_2; [147,148]). In *C. nodosa* rhizome the APX activity measured was greater in plants at the low and medium IBU concentration than in controls and in plants at the high concentration (Fig. 11). However, the activity of POX was significantly reduced while that of CAT was significantly enhanced at the high concentration compared to control (Fig. 11). Since no membrane damage was detected in the rhizome, the slight increase in activity of APX (for plants at the low and medium concentration) and CAT (for plants at the high concentration) might have limited the oxidative stress. It is worth noting that, even with low concentrations of IBU, the activity of antioxidant enzymes such as APX per leaf and rhizome, and POX per leaf, increased. Thus, these physiological parameters may be sensitive enough to detect the toxic effects of environmental stressors and can serve as potential indicators as suggested by Yuan et al. [149].

A significant effect of IBU was also observed on the photosynthetic pigments (Fig. 12). The concentration of chlorophyll b, total chlorophyll, and carotenoids in plants exposed to the high IBU concentration was significantly higher compared to that of plants assigned to other treatments (Fig. 12). The increase in chlorophyll b is of particular interest, and it could be an attempt of plants to increase the ability to harvest light in the restrictive conditions induced by stress. However, a greater availability of chlorophyll could increase the probability of photoinhibition [150], and the increase of carotenoids might be an attempt to protect the photosynthetic apparatus. In contrast with our findings, no changes in the photosynthetic pigment concentration were detected in *Lemna gibba* L. following the exposure to 1 mg L^{-1} of IBU [151]. This suggests a greater sensitivity of *C. nodosa* to IBU contamination compared to freshwater plants.

3.4. Chlorophyll *a* fluorescence transient kinetics

Some pollutants have been found to negatively affect the photosynthetic parameters used as markers of phytotoxicity [65]. In the present work, the analysis of the fast fluorescence kinetics was carried out to determine the effects of IBU on the photosynthetic efficiency of *C. nodosa,* and data interpretation was based primarily on Krüger et al. [152], Paunov et al. [118], Tsimilli-Michael [153] and Zagorchev et al. [154]. Analysis of data from the JIP test conducted at the beginning of the experiment (T0) and after 1 day of exposure (T1) did not demonstrate any significant difference among control and IBU treated plants, therefore these data are not shown. Conversely, the statistical analyses on JIP parameters measured after 5 and 12 days of exposure (at T5 and T12) revealed significant differences between controls and plants exposed to the high IBU concentration. This suggests a certain level of plant tolerance only to low and medium IBU concentration.

At T5, plants exposed to high IBU concentration displayed differences from controls (Fig. 13a), with some parameters demonstrating the onset of a state of stress and others indicating some apparently positive effects. The stress was detectable in the greater dissipation of chlorophyll excitation energy (F_O/F_M and DI_0/RC) and lower efficiency of the Hill reaction (F_V/F_O and $\varphi(P_0)/(1-\varphi(P_0))$ probably due to a damage of the oxygen evolving complex, OEC [155]. The most obvious symptom of the onset of the stress was probably the decrease in the number of active reaction centers per cross section of excited PSII (RC/CS_M) and of their maximum quantum yield of primary photochemistry (F_V/F_M and $\varphi(P_0)$). The greater values of multiple parameters seem to suggest an apparent positive effect of IBU. These values probably indicated an increased energy flux in the intersystem (ET_0/RC) and on the acceptor side of PSI (RE_0/RC), as well as the efficiencies with which the electrons were transferred through these sections of the transport chain ($\psi(E_0)$, $\psi(E_0)/(1-\psi(E_0))$, $\psi(R_0)$, $\delta(R_0)$, $\delta(R_0)/(1-\delta(R_0))$). This may be the consequence of an increased photosynthetic cyclic and pseudocyclic electron flow around PSI (CEF and PEF, respectively), which are known to help generate a ΔpH across the thylakoid membranes enhancing a

Table 3
Summary of the main effects observed in *Cymodocea nodosa* plants exposed to different concentrations of IBU (0.25 μg L^{-1} or Low, 2.5 μg L^{-1} or Medium, 25 μg L^{-1} or High). "= ", "+ ", and "-" indicate an equal, increased, or decreased response compared to that observed in control plants (i.e., 0 μg L^{-1} or no IBU).

	Low(0.25 μg L^{-1})	Medium(2.5 μg L^{-1})	High(25 μg L^{-1})
Morphological and growth traits	=	=	=
Specialized metabolites	=	+ *p*-dihydrocoumaric acid derivate	- total phenolic acids and flavonoids + rutin, gallic acid, *p*-coumaric acid, *p*-dihydrocoumaric acid
		- coumaroyl hexoside II, feruloylhexoside, p-coumaroylmalic acid feruloylmalic acid Hydroxymethylbenzoic acid derivate	- hydroxybenzoic acid derivates, dihydroxybenzoic acid hexoside, hydromethyl benzoic acid derivate, *p*-coumaroyl hexoside I and II feruloyltartaric acid, feruloylhexoside, *p*-coumaroylmalic acid, chicoric acid, caftaric acid, feruloylmalic acid, *p*-dicoumaroyltartaric acid, kaempferol hexoside, isorhamnetin acetylhexoside, isorhamnetin malonylhexoside
Oxidative stress markers	rhizome: = H_2O_2 H_2O_2 in the outer cortical tissue TBARS signal in vascular cortical bundles	rhizome: - H_2O_2 H_2O_2 in the outer and inner cortical tissue TBARS signal in vascular cortical bundles	rhizome: = H_2O_2 H_2O_2 in the outer and inner cortical tissue TBARS signal in vascular cortical bundles and internal cortical tissue
	leaves: + H_2O_2 intensely dark-brown stained	leaves: + H_2O_2 intensely dark-brown stained	leaves: + H_2O_2 intensely dark-brown stained
	+ TBARS	= TBARS	+ TBARS
Antioxidant enzyme activity	rhizome: + APX = POX, SOD - CAT	rhizome: + APX = POX, CAT, SOD	rhizome: = APX, SOD + CAT - POX
	leaves: + APX, POX = CAT, SOD	leaves: + APX = POX, CAT, SOD	leaves: - APX, POX = CAT, SOD
Photosynthetic pigments	= chlorophyll a, b, total, carotenoids	= chlorophyll a, b, total, carotenoids	= chlorophyll a + chlorophyll b, total, carotenoids
Chlorophyll a fluorescence transient kinetics	=	=	+ dissipation of chlorophyll excitation energy (F_O/F_M, DI_0/RC, DI_0/CS_O, DI_0/CS_M) - active RCs (RC/CS_O, RC/CS_M, $\gamma(RC)/(1-\gamma(RC))$) - active OECs ($F_v/F_o$, $\varphi(P_0)/(1-\varphi(P_0))$, V_K) - maximum quantum yield of primary photochemistry of PSII + energy flux in the final part of electron transport chain

non-radiative dissipation of light energy [156]. This interpretation is supported by the high dissipation of excitation energy (F_O/F_M and DI_0/RC) recorded in treated plants. A further apparent beneficial effect arising from an enhanced PEF may be the increase of antioxidant enzymes activity and of antioxidant molecules concentration [157]. Nevertheless, these positive responses were not sufficient to counteract the progress of stress.

At T12, the JIP test highlighted a worsening of the photochemical efficiency (Fig. 13b,c). As occurred at T5, the IBU treatment induced a greater dissipation of chlorophyll excitation energy (F_O/F_M, DI_0/RC, DI_0/CS_O and DI_0/CS_M). It is reasonable to assume that during the experiment the plants were not able to regulate the light energy absorption adjusting the size of their antennas. This is suggested by the values of ABS/CS_O (Fig. 13b) and ABS/CS_M: the former parameter was about 1.5-fold greater than control, while the latter did not differ. This agrees with the observed increase of chlorophyll b concentration in IBU treated plants. Consequently, under IBU treatment the photon absorption continued while the functioning of RCs was severely hindered. The value of ABS/RC, in fact (Fig. 13c), was primarily the consequence of the inactivation of many RCs. This process is confirmed by RC/CS_O, RC/CS_M and $\gamma(RC)/(1-\gamma(RC))$ that in treated *C. nodosa* were half, or even less, compared to control (Fig. 13b). The residual active RCs showed a lower maximum quantum yield of the primary photochemistry of PSII (F_V/F_M and $\varphi(P_0)$; Fig. 13b). The OECs appeared to be more severely damaged than at T5, because in addition to lower F_V/F_O and $\varphi(P_0)/(1-\varphi(P_0))$, the JIP test also detected a higher V_K (Fig. 13b). The decrease in the number of active RCs explains why some parameters seemed to indicate some positive effect of IBU. The number of electron transporters per chain (S_M), the turnover rate of RCs (N) and their average excitation energy ($S_M/t(F_M)$) (Fig. 13c), as well as the trapping of excitons (TR_0/RC) (Fig. 13b) were higher in IBU-exposed plants simply because these parameters refer to active RCs only. Actually, the few active RCs were exposed to a stronger flux of photon energy from the antennas, whose dimensions had not changed from the start of the experiment, suggesting that they were not affected by IBU. In fact, both the trapping of excitons (TR_0/CS_M) and the electron flux in the intersystem per cross section of excited PSII (ET_0/CS_M) (Fig. 13b) were lower in treated *C. nodosa* plants, because of the decreased energy input into the photosynthetic transport chain consequent to the inactivation of many RCs. All the negative effects described so far can also explain the lower PI_{ABS} (performance index of energy conservation of photons absorbed until Q_B reduction) of the treated plants (Fig. 13b). Overall, these results indicate that the main targets of the toxic action of IBU were PSII and its donor side with damages to RCs and to OECs. These results agree with those of a previous study investigating the effects of IBU (3 or 30 mg L^{-1}) on *S. alba* plants grown hydroponically in which the impairment of PSII RCs and the overexcitation of the photochemical system caused the decline of ΦPSII, F_V/F_M, qP and an increase of NPQ, probably due to the generation of reactive radicals [65]. On the other hand, they were not consistent with another study that did not find any changes in the values of F_V/F_M, ΦPSII, qP and ETR in *L. gibba* plants following the exposure to 20, 200 or 1000 μg L^{-1} IBU for 8 days [122]. It is worth noting that, in most cases, both *S. alba* and *L. gibba* had been exposed to IBU concentrations that were higher than those applied in the present work on *C. nodosa*, whose sensitivity and vulnerability to IBU and, probably, to its metabolites are far greater than in the above-mentioned species. As observed at T5, a set of parameters ($(RE_0/CS_O$, φR_0, $\delta(R_0)/(1-\delta(R_0))$ and $\psi(E_0)/(1-\psi(E_0))$) demonstrated that the energy flux in the final part of the photosynthetic electron transport chain and, secondarily, in the intersystem, was greater and more efficient in *C. nodosa* treated plants (Fig. 13c). This cannot be attributed, as it was with RC-based parameters, to the decline of the number of active RCs, perhaps with the only exception of RE_0/RC (Fig. 13c). The greater energy flux in the final section of the transport chain may be the consequence of increased photosynthetic CEF and PEF around PSI, probably a plant response aimed at accelerating energy dissipation. However, PEF did not strengthen antioxidant defenses, because the related enzymes only showed a decline of APX and POX activity and plants exhibited oxidative damage as revealed by the levels of TBARS. Based on our findings, the disturbance of the functioning of the photosynthetic machinery could be considered as an early warning signal of plant damage due to IBU exposure. Thus, the analysis of fast fluorescence kinetics as well as that of antioxidant enzymes may be

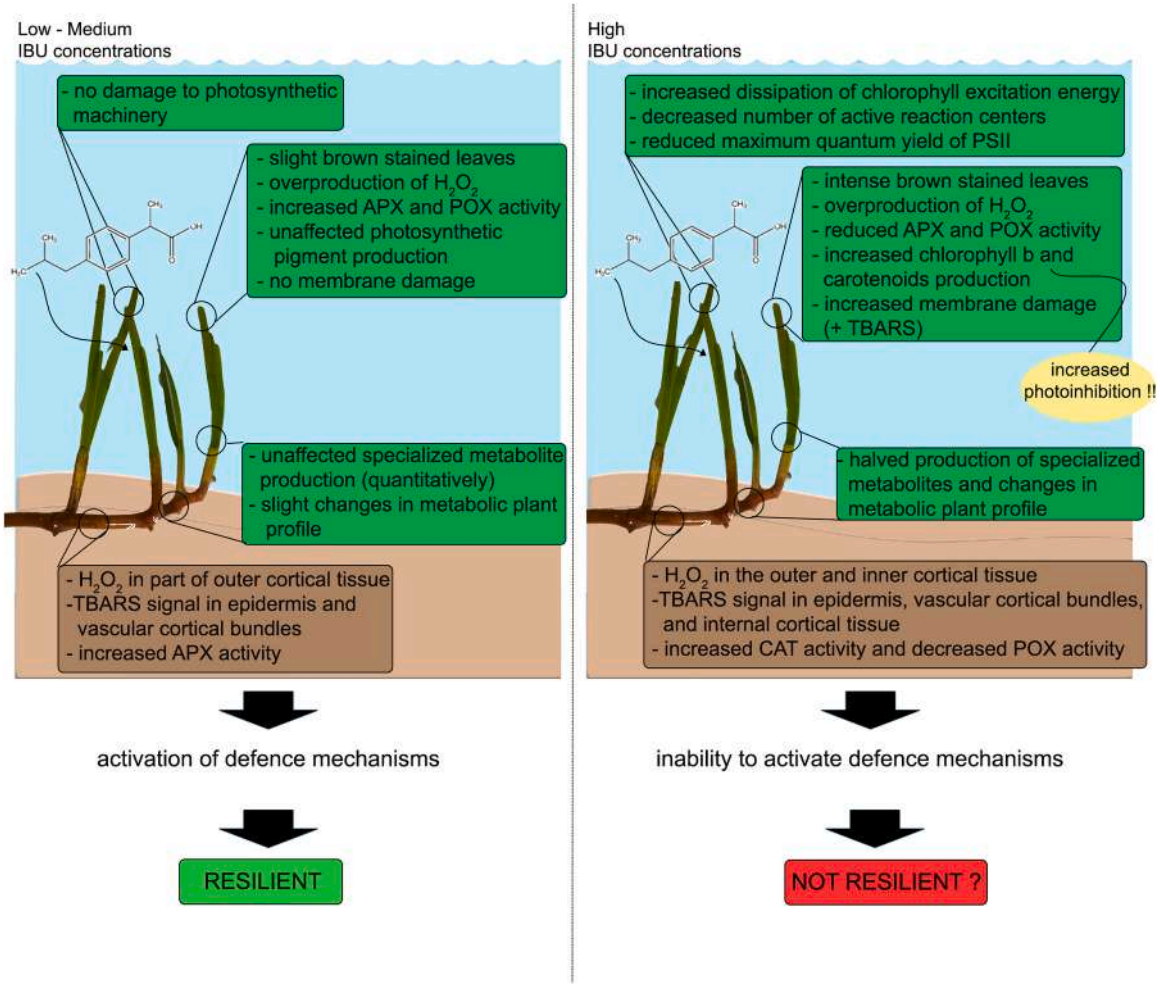

Fig. 14. Graphical representation of the main effects observed in *Cymodocea nodosa* plants exposed to IBU.

effective in monitoring the impact of this pollutant on *C. nodosa.*

3.5. Ecological implications

Our study demonstrates the occurrence of early warning symptoms of damage in *C. nodosa* plants exposed to different environmentally relevant concentrations of IBU for 12 days. Specifically, it shows that at low and medium concentrations, the oxidative stress induced by IBU was counteracted by an increased activity of antioxidant enzymes, like APX and POX, and by the production of specialized metabolites which prevented damage to the photosynthetic machinery (Table 3, Fig. 14). Instead, at the highest IBU concentration the defense activity of antioxidant enzymes as well as the production of specialized metabolites were insufficient to mitigate IBU stress resulting in membrane damage (Table 3, Fig. 14). These findings are of great ecological and managerial value since they inform on the potential risks posed by an increased introduction of IBU in coastal waters due to its growing consumption to seagrass habitats. Indeed, this contaminant could impair *C. nodosa* development and reduce the capacity of plants to cope with other contaminants (e.g., bisphenol A, metal nanoparticles, and micro- and nanoplastics) and climate change-related stressors (e.g., ocean acidification, warming, and eutrophication), possibly leading to the regression of meadows with negative consequences on the ecological functions and services they provide. Thus, more effective conservation strategies involving joint terrestrial and marine-based actions are needed to reduce the introduction of IBU as well as other Phs in marine environments. Terrestrial-based interventions should focus on improving the current removal technologies within wastewater treatment plants and establishing strict regulations on the discharge limits from effluents into surface waters. At the same time, marine-based interventions should include the monitoring of Phs in seagrass habitats and the assessment of thresholds of seagrass tolerance. This latter information could contribute to set regulatory limits for these contaminants in coastal seawaters. Lastly, expanding the current knowledge on the toxicity of Phs to other non-target marine macrophytes and identify those species eventually able to bioaccumulate and degrade these contaminants is also crucial.

4. Conclusions

The presence of Phs in marine environments has been reported, but their effects on seagrasses, which form one of the most valuable ecosystems in the world, have been largely neglected so far. Our study demonstrates that a short-term exposure of the seagrass *C. nodosa* to IBU concentrations currently detected in coastal seawaters may cause oxidative stress. The activation of general defense mechanisms induced by IBU stress may be effective in preventing severe damage indicating plant resilience against this contaminant at concentrations in the range of 0.25–2.5 μg L^{-1}. Instead, they may be insufficient to mitigate the extensive damage to the photosynthetic apparatus and the membrane occurring at higher IBU concentrations. Further studies are needed to evaluate the potential risks of a prolonged exposure to IBU for seagrass resilience against other environmental stressors acting simultaneously or sequentially. This information would be critical in developing

effective seagrass conservation strategies and coastal habitat management actions.

Environmental implication

Pharmaceuticals, such as ibuprofen, are considered emerging contaminants due to their potential adverse effects on marine wildlife. This mesocosm study is the first documenting the effects of environmentally relevant concentrations of ibuprofen detected in the Mediterranean Sea on marine plants (seagrasses), which play fundamental ecological roles, at multiple levels. It shows that short-term exposure of Cymodocea nodosa plants to ibuprofen, especially at the highest concentration, caused oxidative stress and photosynthetic machinery damage. These findings provide valuable insights to assess the potential risk posed by a prolonged exposure of seagrasses to this pollutant and their resilience against environmental stressors.

CRediT authorship contribution statement

Virginia Menicagli: Methodology, Formal analysis, Investigation (plant harvesting, plant cultivation, morphological trait and growth measurements), Visualization, Writing - Review & Editing. **Monica Ruffini Castiglione:** Methodology, Formal analysis, Investigation (plants histochemical assay), Visualization, Writing- Review & Editing, Funding acquisition. **Emily Cioni:** Methodology, Formal analysis, Investigation (detection of IBU in plants and NSW, specialized plant metabolites), Visualization, Writing- Review & Editing. **Carmelina Spanò:** Methodology, Formal analysis, Investigation (oxidative stress evaluation, photosynthetic pigments measurement, antioxidant enzyme activity), Visualization, Writing - Review & Editing, Funding acquisition. **Elena Balestri:** Conceptualization, Methodology, Formal analysis, Investigation (plant harvesting, plant cultivation, morphological trait and growth measurements), Visualization, Supervision, Writing - Review & Editing, Funding acquisition. **Marinella De Leo:** Methodology, Formal analysis, Investigation (detection of IBU in plants and NSW, specialized plant metabolites), Visualization, Writing- Review & Editing, Funding acquisition. **Stefania Bottega:** Methodology, Formal analysis, Investigation (oxidative stress evaluation, photosynthetic pigments measurement, antioxidant enzyme activity), Visualization, Writing - Review & Editing. **Carlo Sorce:** Methodology, Formal analysis, Investigation (photosynthetic efficiency measurements), Visualization, Writing - Review & Editing, Funding acquisition. **Claudio Lardicci:** Conceptualization, Methodology, Formal analysis, Investigation (plant harvesting, plant cultivation, morphological trait and growth measurements), Writing – Review & Editing, Supervision, Funding acquisition.

Declaration of Competing Interest

The authors declare that they have no known competing financial interests or personal relationships that could have appeared to influence the work reported in this paper.

Data Availability

Data will be made available on request.

Acknowledgements and funding

We thank Giada Bernardini for her help in the experiment. We also thank the anonymous referees for their valuable suggestions that improved greatly the quality of the manuscript. This work was funded by Fondi di Ateneo (FA) of University of Pisa (Italy), and by the Italian Ministry of Universities and Research under the Department of Excellence 2023–2027 initiative.

Appendix A. Supporting information

Supplementary data associated with this article can be found in the online version at doi:10.1016/j.jhazmat.2024.135188.

References

[1] Ankley, G.T., Brooks, B.W., Huggett, D.B., Sumpter, J.P., 2007. Repeating history: pharmaceuticals in the environment. Environ Sci Technol 41, 8211–8217. https://doi.org/10.1021/es072658j.

[2] Arrigo, F., De Marchi, L., Meucci, V., Piccione, G., Soares, A.M.V.M., Faggio, C., Freitas, R., 2024. *Mytilus galloprovincialis*: A valuable bioindicator species for understanding the effects of diclofenac under warming conditions (In press.). Sci Total Environ. https://doi.org/10.1016/j.scitotenv.2024.173809.

[3] Blasco, J., Trombini, C., 2023. Ibuprofen and diclofenac in the marine environment - a critical review of their occurrence and potential risk for invertebrate species. Water Emerg Contam Nanoplastics 2, 14. https://doi.org/10.20517/wecn.2023.06.

[4] Branchet, P., Arpin-Pont, L., Pirama, A., Boissery, P., Wong-Wah-Chung, P., Doumenq, P., 2021. Pharmaceuticals in the marine environment: What are the present challenges in their monitoring? Sci Total Environ 766, 142644. https://doi.org/10.1016/j.scitotenv.2020.142644.

[5] Duchet, C., Grabicová, K., Kolar, V., Lepsová, O., Svecová, H., Csercsa, A., Zdvihalová, B., Randák, T., Boukal, D.S., 2024. Combined effects of climate warming and pharmaceuticals on a tri-trophic freshwater food web. Water Res 250, 121053. https://doi.org/10.1016/j.watres.2023.121053.

[6] Ibanez, M., Bijlsma, L., Pitarch, E., López, F.J., Hernández, F., 2021. Occurrence of pharmaceutical metabolites and transformation products in the aquatic environment of the Mediterranean area. Trends Environ Anal Chem 29, e00118. https://doi.org/10.1016/j.teac.2021.e00118.

[7] Kock, A., Glanville, H.C., Law, A.C., Stanton, T., Carter, L.J., Taylor, J.C., 2023. Emerging challenges of the impacts of pharmaceuticals on aquatic ecosystems: A diatom perspective. Sci Total Environ 878, 162939. https://doi.org/10.1016/j.scitotenv.2023.162939.

[8] Mezzelani, M., Nardi, A., Bernardini, I., Milan, M., Peruzza, L., d'Errico, G., Fattorini, D., Gorbi, S., Patarnello, T., 2021. Environmental pharmaceuticals and climate change: The case study of carbamazepine in. *M Gallo* Ocean Acidif Scenar Environ Int 146, 106269. https://doi.org/10.1016/j.envint.2020.106269.

[9] Zhou, Q., Wang, S., Liu, J., Hu, X., Liu, Y., He, Y., He, X., Wu, X., 2022. Geological evolution of offshore pollution and its long-term potential impacts on marine ecosystems. Geosci Front 13, 101427. https://doi.org/10.1016/j.gsf.2022.101427.

[10] Barbier, E.B., Hacker, S.D., Kennedy, C., Koch, E.W., Stier, A.C., Silliman, B., 2011. The value of estuarine and coastal ecosystem services. Ecol Monogr 81, 169–193. https://doi.org/10.1890/10-1510.1.

[11] Henderson, C.J., Stevens, T., Lee, S.Y., Gilby, B.L., Schlacher, T.A., Connolly, R. M., Warnken, J., Maxwell, P.S., Olds, A.D., 2019. Optimising seagrass conservation for ecological functions. Ecosyst 22, 1368–1380. https://doi.org/10.1007/s10021-019-00343-3.

[12] García-Marquez, M.G., Rodríguez-Castañeda, J.C., Agawin, N.S.R., 2023. Sunscreen exposure interferes with physiological processes while inducing oxidative stress in seagrass *Posidonia oceanica* (L.) Delile. Mar Pollut Bull 187, 114507. https://doi.org/10.1016/j.marpolbul.2022.114507.

[13] Lewis, M.A., Devereux, R., 2009. Non nutrient anthropogenic chemicals in seagrass ecosystems: fate and effects. Environ Toxicol Chem (3), 644–661. https://doi.org/10.1897/08-201.1.

[14] Li, Y., Chen, F., Zhou, R., Zheng, X., Pan, K., Qiu, G., Wu, Z., Chen, S., Wang, D., 2023. A review of metal contamination in seagrasses with an emphasis on metal kinetics and detoxification. J Hazard Mater 454, 131500. https://doi.org/10.1016/j.jhazmat.2023.131500.

[15] Long, B.M., Harriage, S., Schultz, N.L., Sherman, C.D.H., Thomas, M., 2023. Pharmaceutical pollution in marine waters and benthic flora of the southern Australian coastline. Environ Chem 19, 375–384. https://doi.org/10.1071/EN22054.

[16] Ralph, P.J., Tomasko, D., Moore, K., Seddon, S., Macinnis-Ng, C.M., 2006. Human impacts on seagrasses: Eutrophication, sedimentation and contamination. In: Larkum, A.W.D., Orth, R.J., Duarte, C.M. (Eds.), 2006. Seagrasses: biology, ecology and conservation. Springer, Dordrecht. https://doi.org/10.1007/978-1-4020-2983-7.

[17] Alfonso-Muniozguren, P., Serna-Galvis, E.A., Bussemaker, M., Torres-Palma, R.A., Lee, J., 2021. A review on pharmaceuticals removal from waters by single and combined biological, membrane filtration and ultrasound systems. Ultrason Sonochem 76, 105656. https://doi.org/10.1016/j.ultsonch.2021.105656.

[18] Madikizela, L.M., Ncube, S., Tutu, H., Richards, H., Newman, B., Ndungu, K., Chimuka, L., 2020. Pharmaceuticals and their metabolites in the marine environment: Sources, analytical methods and occurrence. Trends Environ Anal Chem 28, e00104. https://doi.org/10.1016/j.teac.2020.e00104.

[19] Adeleye, A.S., Xue, J., Zhao, Y., Taylor, A.A., Zenobio, J.E., Sun, Y., Han, Z., Salawu, O.A., Zhu, Y., 2022. Abundance, fate, and effects of pharmaceuticals and personal care products in aquatic environments. J Hazard Mater 424, 127284. https://doi.org/10.1016/j.jhazmat.2021.127284.

[20] EU, 2013. Directive 2013/39/EU of the European Parliament and of the Council of 12 August 2013 amending Directives 2000/60/EC and 2008/105/EC as regards priority substances in the field of water policy.

[21] Ali, A.M., Rønning, H.T., Sydnes, L.K., Alarif, W.M., Kallenborn, R., Al-Lihaibi, S. S., 2018. Detection of PPCPs in marine organisms from contaminated coastal waters of the Saudi Red Sea. Sci Total Environ 621, 654–662. https://doi.org/10.1016/j.scitotenv.2017.11.298.

[22] Álvarez-Muñoz, D., Rodríguez-Mozaz, S., Maulvault, A.L., Tediosi, A., Fernández-Tejedor, M., Van den Heuvel, F., Kotterman, M., Marques, A., Barceló, D., 2015. Occurrence of pharmaceuticals and endocrine disrupting compounds in macroalgaes, bivalves, and fish from coastal areas in Europe. Environ Res 143, 56–64. https://doi.org/10.1016/j.envres.2015.09.018.

[23] Maranho, L.A., DelValls, T.A., Martín-Díaz, M.L., 2015. Assessing potential risks of wastewater discharges to benthic biota: an integrated approach to biomarker responses in clams (*Ruditapes philippinarum*) exposed under controlled conditions. Mar Pollut Bull 92, 11–24. https://doi.org/10.1016/j.marpolbul.2015.01.009.

[24] Świacka, K., Maculewicz, J., Smolarz, K., Szaniawska, A., Caban, M., 2019. Mytilidae as model organisms in themarine ecotoxicology of pharmaceuticals - a review. Environ Pollut 254, 113082. https://doi.org/10.1016/j.envpol.2019.113082.

[25] Almeida, A., Sole, M., Soares, A.M.V.M., Freitas, R., 2020. Anti-inflammatory drugs in the marine environment: Bioconcentration, metabolism and sub-lethal effects in marine bivalves. Environ Pollut 263, 114442. https://doi.org/10.1016/j.envpol.2020.114442.

[26] de Orte, M.R., Carballeira, C., Viana, I.G., Carballeira, A., 2013. Assessing the toxicity of chemical compounds associated with marine land-based fish farms: The use of miniscale microalgal toxicity tests. Chem Ecol 29, 554–563. https://doi.org/10.1080/02757540.2013.790381.

[27] Gonzales-Rey, M., Bebianno, M.J., 2011. Non-steroidal anti-inflammatory drug (NSAID) ibuprofen distresses antioxidant defense system in mussel *Mytilus galloprovincialis* gills. Aquat Toxicol 105, 264–269. https://doi.org/10.1016/j.aquatox.2011.06.015.

[28] Matozzo, V., Rova, S., Marin, M.G., 2012. The nonsteroidal anti-inflammatory drug, ibuprofen, affects the immune parameters in the clam *Ruditapes philippinarum*. Mar Environ Res 79, 116–121. https://doi.org/10.1016/j.marenvres.2012.06.003.

[29] Mezzelani, M., Regoli, F., 2022. The biological effects of pharmaceuticals in the marine environment. Ann Rev Mar Sci 14, 105–128. https://doi.org/10.1146/annurev-marine-040821075606.

[30] Mezzelani, M., Gorbi, S., Fattorini, D., d'Errico, G., Consolandi, G., Milan, M., Bargelloni, L., Regoli, F., 2018. Long-term exposure of *Mytilus galloprovincialis* to diclofenac, Ibuprofen and Ketoprofen: Insights into bioavailability, biomarkers and transcriptomic changes. Chemosphere 198, 238–248. https://doi.org/10.1016/j.chemosphere.2018.01.148.

[31] Silva, M., Feijão, E., da Cruz de Carvalho, R., Duarte, I.A., Matos, A.R., Cabrita, M. T., Barreiro, A., Lemos, M.F.L., Novais, S.C., Marques, J.C., Caçador, I., Reis-Santos, P., Fonseca, V.F., Duarte, B., 2020. Comfortably numb: Ecotoxicity of the non-steroidal anti-inflammatory drug ibuprofen on *Phaeodactylum tricornutum*. Mar Environ Res 161, 105109. https://doi.org/10.1016/j.marenvres.2020.105109.

[32] Świacka, K., Maculewicz, J., Kowalska, D., Caban, M., Smolarz, K., Świezak, J., 2022. Presence of pharmaceuticals and their metabolites in wild-living aquatic organisms – Current state of knowledge. J Hazard Mat 424, 127350. https://doi.org/10.1016/j.jhazmat.2021.127350.

[33] Boudouresque, C.F., Bernard, G., Pergent, G., Shili, A., Verlaque, M., 2009. Regression of Mediterranean seagrasses caused by natural processes and anthropogenic disturbances and stress: a critical review. Bot Mar 395–418. https://doi.org/10.1515/BOT.2009.057.

[34] McMahon, K., Kilminster, K., Canto, R., Roelfsema, C., Lyons, M., Kendrick, G.A., Waycott, M., Udy, J., 2022. The risk of multiple anthropogenic and climate change threats must be considered for continental scale conservation and management of seagrass habitat. Front Mar Sci 9, 837259. https://doi.org/10.3389/fmars.2022.837259.

[35] Smale, D.A., Wernberg, T., Oliver, E.C.J., Thomsen, M., Harvey, B.P., Straub, S.C., Burrows, M.T., Alexander, L.V., Benthuysen, J.A., Donat, M.G., Feng, M., Hobday, A.J., Holbrook, N.J., Perkins-Kirkpatrick, S.E., Scannell, H.A., Sen Gupta, A., Payne, B.L., Moore, P.J., 2019. Marine heatwaves threaten global biodiversity and the provision of ecosystem services. Nat Clim Chang 9, 306–312. https://doi.org/10.1038/s41558-019-0412-1.

[36] Tuya, F., Ribeiro-Leite, L., Arto-Cuesta, N., Coca, J., Haroun, R., Espino, F., 2014. Decadal changes in the structure of *Cymodocea nodosa* seagrass meadows: Natural vs. human influences. Estuar Coast Shelf Sci 137, 41–49. https://doi.org/10.1016/j.ecss.2013.11.026.

[37] Marbà, N., Krause-Jensen, D., Alcoverro, T., Birk, S., Pedersen, A., Neto, J.M., Orfanidis, S., Garmendia, J.M., Muxika, I., Borja, A., Dencheva, K., Duarte, C.M., 2013. Diversity of European seagrass indicators: patterns within and across regions. Hydrobiologia 14 (1). https://doi.org/10.1007/s10750-012-1403-7.

[38] Montefalcone, M., 2009. Ecosystem health assessment using the Mediterranean sea-grass *Posidonia oceanica*: a review. Ecol Indic 9, 595–604. https://doi.org/10.1016/j.ecolind.2008.09.013.

[39] Malea, P., Adamakis, I.-D.S., Kevrekidis, T., 2013. Kinetics of cadmium accumulation and its effects on microtubule integrity and cell viability in the seagrass *Cymodocea nodosa*. Aquat Toxicol 144–145, 257–264. https://doi.org/10.1016/j.aquatox.2013.10.017.

[40] Moustakas, M., Malea, P., Haritonidou, K., Sperdouli, I., 2017. Copper bioaccumulation, photosystem II functioning, and oxidative stress in the seagrass *Cymodocea nodosa* exposed to copper oxide nanoparticles. Environ Sci Pollut Res 24, 16007–16018. https://doi.org/10.1007/s11356-017-9174-3.

[41] Orlando-Bonaca, M., Francé, J., Mavric, B., Grego, M., Lipej, L., Flander-Putrle, V., Sisko, M., Falace, A., 2015. A new index (MediSkew) for the assessment of the *Cymodocea nodosa* (Ucria) Ascherson meadow's status. Mar Environ Res 110, 132–141. https://doi.org/10.1016/j.marenvres.2015.08.009.

[42] Adamakis, I.-D.S., Malea, P., Panteris, E., 2018. The effects of Bisphenol A on the seagrass *Cymodocea nodosa*: Leaf elongation impairment and cytoskeleton disturbance. Ecotoxicol Environ Saf 157, 431–440. https://doi.org/10.1016/j.ecoenv.2018.04.005.

[43] Adamakis, I.-D.S., Malea, P., Sperdouli, I., Panteris, E., Kokkinidi, D., Moustakas, M., 2021. Evaluation of the spatiotemporal effects of bisphenol A on the leaves of the seagrass *Cymodocea nodosa*. J Hazard Mater 404, 124001. https://doi.org/10.1016/j.jhazmat.2020.124001.

[44] Menicagli, V., Ruffini Castiglione, M., Balestri, E., Giorgetti, L., Bottega, S., Sorce, C., Spanò, C., Lardicci, C., 2022. Early evidence of the impacts of microplastic and nanoplastic pollution on the growth and physiology of the seagrass *Cymodocea nodosa*. Sci Total Environ 838, 156514. https://doi.org/10.1016/j.scitotenv.2022.156514.

[45] Mylona, Z., Panteris, E., Kevrekidis, T., Malea, P., 2020. Physiological and structural responses of the seagrass *Cymodocea nodosa* to titanium dioxide nanoparticle exposure. Bot Mar 63, 493–507. https://doi.org/10.1515/bot-2020-0047.

[46] Mylona, Z., Panteris, E., Moustakas, M., Kevrekidis, T., Malea, P., 2020. Physiological, structural and ultrastructural impacts of silver nanoparticles on the seagrass *Cymodocea nodosa*. Chemosphere 248, 126066. https://doi.org/10.1016/j.chemosphere.2020.126066.

[47] Malea, P., Kokkinidi, D., Kevrekidou, A., Adamakis, I.-D.S., 2020. Environmentally relevant bisphenol A concentrations effects on the seagrass *Cymodocea nodosa* different parts elongation: perceptive assessors of toxicity. ESPR 27, 7267–7279. https://doi.org/10.1007/s11356-019-07443-6.

[48] Malea, P., Kokkinidi, D., Kevrekidou, A., Adamakis, I.-D.S., 2022. The enzymatic and non-enzymatic antioxidant system response of the seagrass *Cymodocea nodosa* to bisphenol-A toxicity. Int J Mol Sci 23, 1348. https://doi.org/10.3390/ijms23031348.

[49] Ferreira, B.L., Ferreira, D.P., Borges, S.F., Ferreira, A.M., Holanda, F.H., Ucella-Filho, J.G.M., Cruz, R.A.S., Birolli, W.G., Luque, R., Ferreira, I.M., 2023. Diclofenac, ibuprofen, and paracetamol biodegradation: overconsumed non-steroidal anti-inflammatories drugs at COVID-19 pandemic. Front Microbiol 14, 1207664. https://doi.org/10.3389/fmicb.2023.1207664.

[50] Wang, C., Wang, Z., Wang, G., Yiu-Nam Lau, J., Zhang, K., Li, W., 2021. COVID-19 in early 2021: current status and looking forward. Signal Transduct Target Ther 6, 114. https://doi.org/10.1038/s41392-021-00527-1.

[51] Austin, T., Bregoli, F., Höhne, D., Hendriks, A.J., Ragas, A.M.J., 2022. Ibuprofen exposure in Europe; ePiE as an alternative to costly environmental monitoring. Environ Res 209, 112777. https://doi.org/10.1016/j.envres.2022.112777.

[52] Chopra, S., Kumar, D., 2020. Ibuprofen as an emerging organic contaminant in environment, distribution and remediation. Heliyon 6, e04087. https://doi.org/10.1016/j.heliyon.2020.e04087.

[53] Daughton, C.G., 2003. Cradle-to-cradle stewardship of drugs for minimizing their environmental disposition while promoting human health. I. Rationale for and avenues toward a green pharmacy. EHP 111, 757–774. https://doi.org/10.1289/ehp.5947.

[54] Rainsford, K.D., 2009. Ibuprofen: pharmacology, efficacy and safety. Inflammopharmacology 17, 275–342. https://doi.org/10.1007/s10787-009-0016-x.

[55] Aguilar-Romero, I., Madrid, F., Villaverde, J., Morillo, E., 2024. Ibuprofen-enhanced biodegradation in solution and sewage sludge by a mineralizing microbial consortium. Shift in associated bacterial communities. J Hazard Mater 464, 132970. https://doi.org/10.1016/j.jhazmat.2023.132970.

[56] Ashfaq, M., Khan, K.N., Saif Ur Rehman, M., Mustafa, G., Faizan Nazar, M., Sun, Q., Iqbal, J., Mulla, S.I., Yu, C.-P., 2017. Ecological risk assessment of pharmaceuticals in the receiving environment of pharmaceutical wastewater in Pakistan. Ecotoxicol Environ Saf 136, 31–39. https://doi.org/10.1016/j.ecoenv.2016.10.029.

[57] Jia, Y., Khanal, S.K., Yin, L., Sun, L., Lu, H., 2021. Influence of ibuprofen and its biotransformation products on different biological sludge systems and ecosystem. Environ Int 146, 106265. https://doi.org/10.1016/j.envint.2020.106265.

[58] Spongberg, A.L., Witter, J.D., AcuCa, J., Vargas, J., Murillo, M., Umana, G., Gomez, E., Perez, G., 2011. Reconnaissance of selected PPCP compounds in Costa Rican surface waters. Water Res 45, 6709–6717. https://doi.org/10.1016/j.watres.2011.10.004.

[59] Stasinakis, A.S., Mermigka, S., Samaras, V.G., Farmaki, E., Thomaidis, N.S., 2012. Occurrence of endocrine disrupters and selected pharmaceuticals in Aisonas River (Greece) and environmental risk assessment using hazard indexes. Environ Sci Pollut Res 19, 1574–1583. https://doi.org/10.1007/s11356-011-0661-7.

[60] Ding, T., Yang, M., Zhang, J., Yang, B., Lin, K., Li, J., Gan, J., 2017. Toxicity, degradation and metabolic fate of ibuprofen on freshwater diatom *Navicula* sp. J Hazard Mater 330, 127–134. https://doi.org/10.1016/j.jhazmat.2017.02.004.

[61] Ruggeri, G., Ghigo, G., Maurino, V., Minero, C., Vione, D., 2013. Photochemical transformation of ibuprofen into harmful 4-isobutylacetophenone: Pathways, kinetics, and significance for surface waters. Water Res 47, 6109–6121. https://doi.org/10.1016/j.watres.2013.07.031.

[62] Vione, D., Reddy Maddigapu, P., De Laurentiis, E., Minella, M., Pazzi, M., Maurino, V., Minero, C., Kouras, S., Richard, C., 2011. Modelling the photochemical fate of ibuprofen in surface waters. Water Res 45, 6725–6736. https://doi.org/10.1016/j.watres.2011.10.014.

[63] Calderón-Preciado, D., Matamoros, V., Bayona, J.M., 2011. Occurrence and potential crop uptake of emerging contaminants and related compounds in an agricultural irrigation network. Sci Total Environ 412-413, 14–19. https://doi.org/10.1016/j.scitotenv.2011.09.057.
[64] He, Y., Langenhoff, A.A.M., Sutton, N.B., Rijnaarts, H.H.M., Blokland, M.H., Chen, F., Huber, C., Schröder, P., 2017. Metabolism of Ibuprofen by *Phragmites australis*: Uptake and phytodegradation. Environ Sci Technol 51, 4576–4584. https://doi.org/10.1021/acs.est.7b00458.
[65] Iori, V., Zacchini, M., Pietrini, F., 2013. Growth, physiological response and phytoremoval capability of two willow clones exposed to ibuprofen under hydroponic culture. J Hazard Mater 262, 796–804. https://doi.org/10.1016/j.jhazmat.2013.09.017.
[66] Li, Y., Zhang, J., Zhu, G., Liu, Y., Wu, B., Ng, W.J., Appan, A., Tanet, S.K., 2016. Phytoextraction, phytotransformation and rhizodegradation of ibuprofen associated with *Typha angustifolia* in a horizontal subsurface flow constructed wetland. Water Res 102, 294–304. https://doi.org/10.1016/j.watres.2016.06.049.
[67] Biel Maeso, M., Baena-Nogueras, R.M., Corada-Fernández, C., Lara-Martín, P.A., 2018. Occurrence, distribution and environmental risk of pharmaceutically active compounds (PhACs) in coastal and ocean waters from the Gulf of Cadiz (SW Spain). Sci Total Environ 612, 649–659. https://doi.org/10.1016/j.scitotenv.2017.08.279.
[68] Brumovský, M., Bečanová, J., Kohoutek, J., Borghini, M., Nizzetto, L., 2017. Contaminants of emerging concern in the open sea waters of the Western Mediterranean. Environ Pollut 229, 976–983. https://doi.org/10.1016/j.envpol.2017.07.082.
[69] Loos, R., Tavazzi, S., Paracchini, B., Canuti, E., Weissteiner, C., 2013. Analysis of polar organic contaminants in surface water of the northern Adriatic Sea by solid-phase extraction followed by ultrahigh-pressure liquid chromatography–QTRAP® MS using a hybrid triple-quadrupole linear ion trap instrument. Anal Bioanal Chem 405, 5875–5885. https://doi.org/10.1007/s00216-013-6944-8.
[70] Togola, A., Budzinski, H., 2008. Multi-residue analysis of pharmaceutical compounds in aqueous samples. J Chromatogr A 1177, 150–158. https://doi.org/10.1016/j.chroma.2007.10.105.
[71] Oh, S., Shin, W.S., Kim, H.T., 2016. Effects of pH, dissolved organic matter, and salinity on ibuprofen sorption on sediment. Environ Sci Pollut Res 23, 22882–22889. https://doi.org/10.1007/s11356-016-7503-6.
[72] Oskarsson, H., Eriksson Wiklund, A.-K., Lindh, K., Kumblad, L., 2012. Effect studies of human pharmaceuticals on *Fucus vesiculosus* and *Gammarus* spp. Mar Environ Res 74, 1–8. https://doi.org/10.1016/j.marenvres.2011.11.001.
[73] Wiklund, A.-K.E., Oskarsson, H., Thorsén, G., Kumblad, L., 2011. Behavioural and physiological responses to pharmaceutical exposure in macroalgae and grazers from a Baltic Sea littoral community. Aquat Biol 14, 29–39. https://doi.org/10.3354/ab00380.
[74] Kuo, J., den Hartog, C., 2006. Seagrass morphology, anatomy, and ultrastructure. In: Larkum, A.W.D., Orth, R.J., Duarte, C.M. (Eds.), 2006. Seagrasses: biology, ecology and conservation. Springer, Dordrecht. https://doi.org/10.1007/978-1-4020-2983-7.
[75] Bayen, S., Zhang, H., Desai, M.M., Ooi, S.K., Kelly, B.C., 2013. Occurrence and distribution of pharmaceutically active and endocrine disrupting compounds in Singapore's marine environment: Influence of hydrodynamics and physical-chemical properties. Environ Poll 182, 1–8. https://doi.org/10.1016/j.envpol.2013.06.028.
[76] Wu, J., Qian, X., Yang, Z., Zhang, L., 2010. Study on the matrix effect in the determination of selected pharmaceutical residues in seawater by solid-phase extraction and ultra-high-performance liquid chromatography–electrospray ionization low-energy collision-induced dissociation tandem mass spectrometry. J Chromatogr A 1217, 1471–1475. https://doi.org/10.1016/j.chroma.2009.12.074.
[77] Gevao, B., Uddin, S., Dupont, S., 2021. Baseline concentrations of pharmaceuticals in Kuwait's coastal marine environment. Mar Pollut Bull 173, 113040. https://doi.org/10.1016/j.marpolbul.2021.113040.
[78] Ngubane, N.P., Naicker, D., Ncube, S., Chimuka, L., Madikizela, L.M., 2019. Determination of naproxen, diclofenac and ibuprofen in Umgeni estuary and seawater: A case of northern Durban in KwaZulu–Natal Province of South Africa. Reg Stud Mar Sci 29, 100675. https://doi.org/10.1016/j.rsma.2019.100675.
[79] Netshithothole, R., Madikizela, L.M., 2024. Occurrence of selected pharmaceuticals in the East London coastline encompassing major rivers, estuaries, and seawater in the Eastern Cape Province of South Africa. ACS Meas Sci Au 4, 283–293. https://doi.org/10.1021/acsmeasuresciau.4c00004.
[80] Fang, T.-H., Nan, F.-H., Chin, T.-S., Feng, H.-M., 2012. The occurrence and distribution of pharmaceutical compounds in the effluents of a major sewage treatment plant in Northern Taiwan and the receiving coastal waters. Mar Pollut Bull 64, 1435–1444. https://doi.org/10.1016/j.marpolbul.2012.04.008.
[81] Jiang, J.-J., Lee, C.-L., Fang, M.-D., 2014. Emerging organic contaminants in coastal waters: Anthropogenic impact, environmental release and ecological risk. Mar Pollut Bull 85, 391–399. https://doi.org/10.1016/j.marpolbul.2013.12.045.
[82] Nödler, K., Voutsa, D., Licha, T., 2014. Polar organic micropollutants in the coastal environment of different marine systems. Mar Pollut Bull 85, 50–59. https://doi.org/10.1016/j.marpolbul.2014.06.024.
[83] Vidal-Dorsch, D.E., Bay, S.M., Maruya, K., Snyder, S.A., Trenholm, R.A., Vanderford, B.J., 2012. Contaminants of emerging concern in municipal wastewater effluents and marine receiving water. Environ Tox Chem 31, 2674–2682. https://doi.org/10.1002/etc.2004.
[84] Ali, A.M., Rønning, H.T., Alarif, W.M., Kallenborn, R., Al-Lihaibi, S.S., 2017. Occurrence of pharmaceuticals and personal care products in effluent dominated Saudi Arabian coastal waters of the Red Sea. Chemosphere 175, 505–513. https://doi.org/10.1016/j.chemosphere.2017.02.095.
[85] Pereira, C.D.S., Maranho, L.A., Cortez, F.S., Pusceddu, F.H., Santos, A.R., Ribeiro, D.A., Cesar, A., Guimarães, L.L., 2016. Occurrence of pharmaceuticals and cocaine in a Brazilian coastal zone. Sci Total Environ 548-549, 148–154. https://doi.org/10.1016/j.scitotenv.2016.01.051.
[86] Lolic, A., Paíga, P., Santos, L.H.M.L.M., Ramos, S., Correia, M., Delerue-Matos, C., 2015. Assessment of non-steroidal anti-inflammatory and analgesic pharmaceuticals in seawaters of North of Portugal: Occurrence and environmental risk. Sci Total Environ 508, 240–250. https://doi.org/10.1016/j.scitotenv.2014.11.097.
[87] Feo, M.L., Bagnati, R., Passoni, A., Riva, F., Salvagio Manta, D., Sprovieri, M., Traina, A., Zuccato, E., Castiglioni, S., 2020. Pharmaceuticals and other contaminants in waters and sediments from Augusta Bay (southern Italy). Sci Total Environ 739, 139827. https://doi.org/10.1016/j.scitotenv.2020.139827.
[88] Gros, M., Rodríguez-Mozaza, S., Barceló, D., 2012. Fast and comprehensive multi-residue analysis of a broad range of human and veterinary pharmaceuticals and some of their metabolites in surface and treated waters by ultra-high-performance liquid chromatography coupled to quadrupole-linear ion trap tandem mass spectrometry. J Chromatogr A 1248, 104–121. https://doi.org/10.1016/j.chroma.2012.05.084.
[89] Korkmaz, N.E., Savun-Hekimoğlu, B., Aksu, A., Burak, S., Balkis Caglar, N., 2022. Occurrence, sources and environmental risk assessment of pharmaceuticals in the Sea of Marmara, Turkey. Sci Total Environ 819, 152996. https://doi.org/10.1016/j.scitotenv.2022.152996.
[90] Weigel, S., Berger, U., Jensen, E., Kallenborn, R., Thoresen, H., Hühnerfuss, H., 2004. Determination of selected pharmaceuticals and caffeine in sewage and seawater from Tromsø/Norway with emphasis on ibuprofen and its metabolites. Chemosphere 56, 583–592. https://doi.org/10.1016/j.chemosphere.2004.04.015.
[91] Letsinger, S., Kaya, P., Rodríguez-Mozaz, S., Villagrassa, M., Barceló, D., Rotchell, J.M., 2019. Spatial and temporal occurrence of pharmaceuticals in UK estuaries. Sci Total Environ 678, 74–84. https://doi.org/10.1016/j.scitotenv.2019.04.182.
[92] Thomas, K.V., Hilton, M.J., 2004. The occurrence of selected human pharmaceutical compounds in UK estuaries. Mar Pollut Bull 49, 436–444. https://doi.org/10.1016/j.marpolbul.2004.02.028.
[93] Gonzalez Rey, M., Tapie, N., Le Menach, K., Dévier, M.-H., Budzinski, H., Bebianno, M.J., 2015. Occurrence of pharmaceutical compounds and pesticides in aquatic systems. Mar Pollut Bull 96, 384–400. https://doi.org/10.1016/j.marpolbul.2015.04.029.
[94] Agostini, S., Pergent, M., Marchard, B., 2003. Growth and primary production of *Cymodocea nodosa* in a coastal lagoon. Aquat Bot 185–193. https://doi.org/10.1016/S0304-3770(03)00049-4.
[95] Alberto, F., Arnaud-Haond, S., Duarte, C.M., Serrão, E.A., 2006. Genetic diversity of a clonal angiosperm near its range limit: the case of *Cymodocea nodosa* at the Canary Islands. Mar Ecol Progr Ser 309, 117–129. https://doi.org/10.3354/meps309117.
[96] Cancemi, G., Buia, M.C., Mazzella, L., 2002. Structure and growth dynamics of *Cymodocea nodosa* meadows. Sci Mar 66, 365–373. https://doi.org/10.3989/scimar.
[97] de los Santos, C., Brun, F.G., Vergara, J.J., Perez-Lloréns, J.L., 2013. New aspect in seagrass acclimation: leaf mechanical properties vary spatially and seasonally in the temperate species *Cymodocea nodosa* Ucria (Ascherson). Mar Biol 160, 1083–1093. https://doi.org/10.1007/s00227-012-2159-3.
[98] Malea, P., Kevrekidis, T., Chatzipanagiotou, K.-R., Mogias, A., 2018. Cadmium uptake kinetics in parts of the seagrass *Cymodocea nodosa* at high exposure concentrations. J Biol Res-Thessalon 25, 5. https://doi.org/10.1186/s40709-018-0076-4.
[99] Menicagli, V., Balestri, E., Vallerini, F., De Battisti, D., Lardicci, C., 2021. Plastics and sedimentation foster the spread of a non-native macroalga in seagrass meadows. Sci Total Environ 757, 143812. https://doi.org/10.1016/j.scitotenv.2020.143812.
[100] Marbà, N., Cebrián, J., Enríquez, S., Duarte, C.M., 1996. Growth patterns of Western Mediterranean seagrasses: species-specific responses to seasonal forcing. Mar Ecol Progr Ser 133, 203–215. https://doi.org/10.3354/meps133203.
[101] Peduzzi, P., Vukovic, A., 1990. Primary production of *Cymodocea nodosa* in the Gulf of Trieste (Northern Adriatic Sea): a comparison of methods. Mar Ecol Progr Ser 64, 197–207.
[102] Sghaier, Y.R., Zakhama-Sraieb, R., Charfi-Cheikhrouha, F., 2011. Primary production and biomass in a *Cymodocea nodosa* meadow in the Ghar El Melh lagoon, Tunisia. Bot Mar 54, 411–418. https://doi.org/10.1515/BOT.2011.045.
[103] Cioni, E., De Leo, M., Cacciola, A., D'Angelo, V., Germanò, M.P., Camangi, F., Ricci, D., Fabene, E., Diretto, G., De Tommasi, N., Braca, A., 2024. Re-discovering *Prunus* fruit varieties as antiangiogenic agents by metabolomic and bioinformatic approach. Food Chem 435, 137574. https://doi.org/10.1016/j.foodchem.2023.137574.
[104] Schymanski, E.L., Jeon, J., Gulde, R., Fenner, K., Ruff, M., Singer, H.P., Hollender, J., 2014. Identifying small molecules via high resolution mass spectrometry: communicating confidence. Environ Sci Technol 48, 2097–2098. https://doi.org/10.1021/es5002105.
[105] Jana, S., Choudhuri, M.A., 1982. Glycolate metabolism of three submersed aquatic angiosperms during ageing. Aquat Bot 12, 345–354. https://doi.org/10.1016/0304-3770(82)90026-2.

[106] Spanò, C., Bottega, S., Ruffini Castiglione, M., Pedranzani, H.E., 2017. Antioxidant response to cold stress in two oil plants of the genus *Jatropha*. Plant Soil Environ 63, 271–276. https://doi.org/10.17221/182/2017-PSE.
[107] Daudi, A., O'Brien, J.A., 2012. Detection of hydrogen peroxide by DAB staining in *Arabidopsis* leaves. Bio Protoc 2, e263.
[108] Yamamoto, Y., Kobayashi, Y., Matsumoto, H., 2001. Lipid peroxidation is an early symptom triggered by aluminum, but not the primary cause of elongation inhibition in pea roots. Plant Physiol 125, 199–208. https://doi.org/10.1104/pp.125.1.199.
[109] Giorgetti, L., Spanò, C., Muccifora, S., Bellani, L., Tassi, E., Bottega, S., Di Gregorio, S., Siracusa, G., Sanità di Toppi, L., Ruffini Castiglione, M., 2019. An integrated approach to highlight biological responses of *Pisum sativum* root to nano-TiO_2 exposure in a biosolid-amended agricultural soil. Sci Tot Environ 650, 2705–2716. https://doi.org/10.1016/j.scitotenv.2018.10.032.
[110] Spanò, C., Bottega, S., Bellani, L., Muccifora, S., Sorce, C., Ruffini Castiglione, M., 2020. Effect of zinc priming on salt response of wheat seedlings: relieving or worsening? Plants 9, 1514. https://doi.org/10.3390/plants9111514.
[111] Spanò, C., Bruno, M., Bottega, S., 2013. *Calystegia soldanella*: dune versus laboratory plants to highlight key adaptive physiological traits. Acta Physiol Plant 35, 1329–1336. https://doi.org/10.1007/s11738-012-1173-x.
[112] Spanò, C., Bottega, S., Lorenzi, R., Grilli, I., 2011. Ageing in embryos from wheat grains stored at different temperatures: oxidative stress and antioxidant response. Funct Plant Biol 38, 624–631. https://doi.org/10.1071/FP11046.
[113] Aebi, H., 1984. Catalase in vitro. Methods Enzym 105, 121–126. https://doi.org/10.1016/S00766879(84)05016-3.
[114] Arezki, O., Boxus, P., Kevers, C., Gaspar, T., 2001. Changes in peroxidase activity, and level of phenolic compounds during light-induced plantlet regeneration from *Eucalyptus camaldulensis* Dehn. nodes in vitro. Plant Growth Regul 33, 215–219. https://doi.org/10.1023/A:1017579623170.
[115] Spanò, C., Bottega, S., 2016. Durum wheat seedlings in saline conditions: salt spray versus root-zone salinity. Estuar Coast Shelf Sci 169, 173–181. https://doi.org/10.1016/j.ecss.2015.11.031.
[116] Bradford, M.M., 1976. A rapid and sensitive method for the quantitation of microgram quantities of protein utilizing the principle of protein-dye binding. Anal Biochem 7, 248–254. https://doi.org/10.1006/abio.1976.9999.
[117] Stirbet, A., Lazár, D., Kromdijk, J., Govindjee, 2018. Chlorophyll a fluorescence induction: Can just a one-second measurement be used to quantify abiotic stress responses? Photosynthetica 56, 86–104. https://doi.org/10.1007/s11099-018-0770-3.
[118] Paunov, M., Koleva, L., Vassilev, A., Vangronsveld, J., Goltsev, V., 2018. Effects of different metals on photosynthesis: Cadmium and Zinc affect chlorophyll fluorescence in durum wheat. Int J Mol Sci 19, 787. https://doi.org/10.3390/ijms19030787.
[119] Sandrini-Neto, L., Camargo, M.G., 2014. GAD: An R Package for ANOVA Designs from general principles. R Package.
[120] Dinno, A., 2015. Nonparametric pairwise multiple comparisons in independent groups using Dunn's test. Stata J 15, 292–300. https://doi.org/10.1177/1536867X1501500117.
[121] R. Core Team, 2018. R: A Language and Environment for Statistical Computing. R Foundation for Statistical Computing, Vienna. https://www.R-project.org.
[122] Di Baccio, D., Pietrini, F., Bertolotto, P., Pérez, S., Barcelò, D., Zacchini, M., Donati, E., 2017. Response of *Lemna gibba* L. to high and environmentally relevant concentrations of ibuprofen: Removal, metabolism and morpho-physiological traits for biomonitoring of emerging contaminants. Sci Total Environ 584-585, 363–373. https://doi.org/10.1016/j.scitotenv.2016.12.191.
[123] Pomati, F., Netting, A.G., Calamari, D., Neilan, B.A., 2004. Effects of erythromycin, tetracycline and ibuprofen on the growth of *Synechocystis* sp. and *Lemna minor*. Aquat Toxicol 67, 387–396. https://doi.org/10.1016/j.aquatox.2004.02.001.
[124] Grignon-Dubois, M., Rezzonico, B., 2013. The economic potential of beach-cast seagrass–*Cymodocea nodosa*: a promising renewable source of chicoric acid. Bot Mar 56, 303–311. https://doi.org/10.1515/bot-2013-0029.
[125] Milović, S., Stanković, I., Nikolić, D., Radović, J., Kolundžić, M., Nikolić, V., Stanojković, T., Petović, S., Kundaković-Vasović, T., 2019. Chemical analysis of selected seaweeds and seagrass from the Adriatic Coast of Montenegro. Chem Biodivers 16, e1900327. https://doi.org/10.1002/cbdv.201900327.
[126] Smadi, A., Ciavatta, M.L., Bitam, F., Carbone, M., Villani, G., Gavagnin, M., 2018. Prenylated flavonoids and phenolic compounds from the rhizomes of marine phanerogam *Cymodocea nodosa*. Planta Med 84, 704–709. https://doi.org/10.1055/s-0043-122747.
[127] Tuladhar, P., Sasidharan, S., Saudagar, P., 2021. Role of phenols and polyphenols in plant defense response to biotic and abiotic stresses. In: Jogaiah, S. (Ed.), Biocontrol agents and secondary metabolites, 2001. Woodhead Publishing, pp. 419–441. https://doi.org/10.1016/B978-0-12-822919-4.00017-X.
[128] Astudillo-Pascual, M., Domínguez, I., Aguilera, P.A., Garrido Frenich, A., 2021. New phenolic compounds in *Posidonia oceanica* seagrass: A comprehensive array using high resolution mass spectrometry. Plants 10, 864. https://doi.org/10.3390/plants10050864.
[129] Carazzone, C., Mascherpa, D., Gazzani, G., Papetti, A., 2013. Identification of phenolic constituents in red chicory salads (*Cichorium intybus*) by high-performance liquid chromatography with diode array detection and electrospray ionisation tandem mass spectrometry. Food Chem 138, 1062–1071. https://doi.org/10.1016/j.foodchem.2012.11.060.
[130] Ostrowski, W., Wojakowska, A., Grajzer, M., Stobiecki, M., 2014. Mass spectrometric behavior of phenolic acids standards and their analysis in the plant samples with LC/ESI/MS system. J Chromatogr B 967, 21–27. https://doi.org/10.1016/j.jchromb.2014.07.005.
[131] López-Fernández, O., Domínguez, R., Pateiro, M., Munekata, P.E., Rocchetti, G., Lorenzo, J.M., 2020. Determination of polyphenols using liquid chromatography–tandem mass spectrometry technique (LC–MS/MS): a review. Antioxidants 9, 479. https://doi.org/10.3390/antiox9060479.
[132] Navarro-Hoyos, M., Arnáez-Serrano, E., Quesada-Mora, S., Azofeifa-Cordero, G., Wilhelm-Romero, K., Quirós-Fallas, M.I., Alvarado-Corella, D., Vargas-Huertas, F., Sánchez-Kopper, A., 2021. Polyphenolic QTOF-ESI MS characterization and the antioxidant and cytotoxic activities of Prunus domestica commercial cultivars from Costa Rica. Molecules 26, 6493. https://doi.org/10.3390/molecules26216493.
[133] Sánchez-Rabaneda, F., Jáuregui, O., Casals, I., Andrés-Lacueva, C., Izquierdo-Pulido, M., Lamuela-Raventós, R.M., 2003. Liquid chromatographic/electrospray ionization tandem mass spectrometric study of the phenolic composition of cocoa (*Theobroma cacao*). J Mass Spectrom 38, 35–42. https://doi.org/10.1002/jms.395.
[134] Navarro, M., Moreira, I., Arnaez, E., Quesada, S., Azofeifa, G., Vargas, F., Alvarado, D., Chen, P., 2018. Polyphenolic characterization and antioxidant activity of *Malus domestica* and *Prunus domestica* cultivars from Costa Rica. Foods 7, 15. https://doi.org/10.3390/foods7020015.
[135] Lijia, X., Guo, J., Chen, Q., Baoping, J., Zhang, W., 2014. Quantitation of phlorizin and phloretin using an ultra high-performance liquid chromatography–electrospray ionization tandem mass spectrometric method. J Chromatogr B 960, 67–72. https://doi.org/10.1016/j.jchromb.2014.04.007.
[136] Rodriguez-Rojas, F., Navarrete, C., Rámila, C., Tapia-Reyes, P., Celis-Plá, P.S.M., González, C., Pereira-Rojas, J., Blanco-Murillo, F., Moreno, P., Gutiérrez-Campos, C., Sánchez-Lizaso, J.L., Sáez, C.A., 2024. Transcriptomic profiles and diagnostic biomarkers in the Mediterranean seagrasses *Posidonia oceanica* and *Cymodocea nodosa* reveal mechanistic insights of adaptative strategies upon desalination brine stress. Sci Total Environ 916, 170326. https://doi.org/10.1016/j.scitotenv.2024.170326.
[137] Gorni, P.H., de Lima, G.R., de Oliveira Pereira, L.M., Spera, K.D., de Marcos Lapaz, A., Pacheco, A.C., 2022. Increasing plant performance, fruit production and nutritional value of tomato through foliar applied rutin. Sci Hortic 294, 110755. https://doi.org/10.1016/j.scienta.2021.110755.
[138] Ismail, H., Maksimović, J.D., Maksimović, V., Shabala, L., Živanović, B.D., Tian, Y., Jacobsen, S.E., Shabala, S., 2015. Rutin, a flavonoid with antioxidant activity, improves plant salinity tolerance by regulating K+ retention and Na+ exclusion from leaf mesophyll in quinoa and broad beans. Func Plant Bio 43, 75–86. https://doi.org/10.1071/FP15312.
[139] Zhang, X., Ran, W., Ye, M., Lin, S., Liu, M., Sun, X., 2022. Exogenous application of gallic acid induces the direct defense of tea plant against *Ectropis obliqua* Caterpillars. Front Plant Sci 13, 833489. https://doi.org/10.3389/fpls.2022.833489.
[140] Yeshi, K., Crayn, D., Ritmejerytė, E., Wangchuk, P., 2022. Plant secondary metabolites produced in response to abiotic stresses has potential application in pharmaceutical product development. Molecules 27 (1), 313. https://doi.org/10.3390/molecules27010313.
[141] Subhashini, P., Dilipan, E., Thangaradjou, T., Papenbrock, J., 2013. Bioactive natural products from marine angiosperms: abundance and functions. Nat Prod Bioprospect 3, 129–136. https://doi.org/10.1007/s13659-013-0043-6.
[142] Wijaya, L., Alyemeni, M., Ahmad, P., Alfarhan, A., Barcelo, D., El-Sheikh, M.A., Pico, Y., 2020. Ecotoxicological effects of Ibuprofen on plant growth of *Vigna unguiculata* L. Plants 9, 1473. https://doi.org/10.3390/plants9111473.
[143] Asaeda, T., Rahman, M., Liping, X., Schoelynck, J., 2022. Hydrogen peroxide variation patterns as abiotic stress responses of *Egeria densa*. Front Plant Sci 13, 855477. https://doi.org/10.3389/fpls.2022.855477.
[144] Noctor, G., Mhamdi, A., Foyer, C.H., 2014. The roles of reactive oxygen metabolism in drought: Not so cut and dried. Plant Physiol 164, 1636–1648. https://doi.org/10.1104/pp.113.233478.
[145] Smirnoff, N., Arnaud, D., 2019. Hydrogen peroxide metabolism and functions in plants. N Phytol 221, 1197–1214. https://doi.org/10.1111/nph.15488.
[146] Mittler, R., 2002. Oxidative stress, antioxidants and stress tolerance. Trends Plant Sci 7, 405–410. https://doi.org/10.1016/S1360-1385(02)02312-9.
[147] Dwivedi, S., Tripathi, R.D., Tripathi, P., Kumar, A.R.D., Mishra, S., Singh, R., Sharma, D., Rai, U.N., Charkrabarty, D., Trivedi, P.K., Adhikari, B., Bag, M.K., Dhankher, O.P., Tuli, R., 2010. Arsenate exposure affects amino acids, mineral nutrient status and antioxidants in rice (*Oryza sativa* L.) genotypes. Environ Sci Technol 44, 9542–9549. https://doi.org/10.1021/es101716h.
[148] Sofo, A., Scopa, A., Nuzzaci, M., Vitti, A., 2015. Ascorbate peroxidase and catalase activities and their genetic regulation in plants subjected to drought and salinity stresses. Int J Mol Sci 16, 13561–13578. https://doi.org/10.3390/ijms160613561.
[149] Yuan, L., Richardson, C.J., Ho, M., Willis, C.W., Colman, B.P., Wiesne, M.R., 2018. Stress responses of aquatic plants to silver nanoparticles. Environ Sci Technol 52, 2558–2565. https://doi.org/10.1021/acs.est.7b05837.
[150] Bascuñán-Godoy, L., Sanhueza, C., Cuba, M., Zuñiga, G.E., Corcuera, L.J., Bravo, L.A., 2012. Cold-acclimation limits low temperature induced photoinhibition by promoting a higher photochemical quantum yield and a more effective PSII restoration in darkness in the Antarctic rather than the Andean ecotype of *Colobanthus quitensis* Kunt Bartl (Cariophyllaceae). BMC Plant Biol 12, 114. https://doi.org/10.1186/1471-2229-12-114.
[151] Pietrini, F., Di Baccio, D., Aceña, J., Pérez, S., Barceló, D., Zacchini, M., 2015. Ibuprofen exposure in *Lemna gibba* L.: Evaluation of growth and phytotoxic indicators, detection of ibuprofen and identification of its metabolites in plant and

in the medium. J Hazard Mater 300, 189–193. https://doi.org/10.1016/j.jhazmat.2015.06.068.

[152] Krüger, G.H.J., De Villiers, M.F., Strauss, A.J., de Beer, M., van Heerden, P.D.R., Maldonado, R., Strasser, R.J., 2014. Inhibition of photosystem II activities in soybean (*Glycine max*) genotypes differing in chilling sensitivity. S Afr J Bot 95, 85–96. https://doi.org/10.1016/j.sajb.2014.07.010.

[153] Tsimilli-Michael, M., 2020. Revisiting JIP-test: An educative review on concepts, assumptions, approximations, definitions and terminology. Photosynthetica 58, 275–292. https://doi.org/10.32615/ps.2019.150.

[154] Zagorchev, L., Atanasova, A., Albanova, I., Traianova, A., Mladenov, P., Kouzmanova, M., Goltsev, V., Kalaji, H.M., Teofanova, D., 2021. Functional characterization of the photosynthetic machinery in smicronix galls on the parasitic plant *Cuscuta campestris* by JIP-Test. Cells 10, 1399. https://doi.org/10.3390/cells10061399.

[155] Gupta, R., 2020. The oxygen-evolving complex: a super catalyst for life on earth, in response to abiotic stresses. Plant Signal Behav 15 (12). https://doi.org/10.1080/15592324.2020.1824721.

[156] Makino, A., Miyake, C., Yokota, A., 2002. Physiological functions of the water–water cycle (Mehler Reaction) and the cyclic electron flow around PSI in rice leaves. Plant Cell Physiol 43, 1017–1026. https://doi.org/10.1093/pcp/pcf124.

[157] Cheng, H., Wang, X., Wang, J., Li, Q., 2021. Key photoprotective pathways of a shade-tolerant plant (*Alpinia oxyphylla*) for precipitation patterns change during the dry season: thermal energy dissipation and water-water cycle. Plant Stress 2, 100016. https://doi.org/10.1016/j.stress.2021.100016.